Estimating large scale land surface fluxes: the use of remote sensing data with SVAT and NWP models

J.D. Kalma, S.W. Franks, B.J.J.M. van den Hurk, M.F. McCabe and R.A. Feddes

RAPPORT 90

Sectie Waterhuishouding
Nieuwe Kanaal 11, 6709 PA Wageningen

ISSN 0926-230X

ESTIMATING LARGE SCALE LAND SURFACE FLUXES: THE USE OF REMOTE SENSING DATA WITH SVAT AND NWP MODELS

J. D. Kalma*, S. W. Franks*, B. J. J. M. van den Hurk , M. F. McCabe* and R. A. Feddes*****

* Department of Civil, Surveying and Environmental Engineering,
University of Newcastle, Callaghan NSW 2308, Australia.

**Atmospheric Research Division,
Royal Netherlands Meteorological Institute, 3730 AE De Bilt, Netherlands.

***Department of Water Resources,
Wageningen University, 6709 PA Wageningen, Netherlands

Abstract

Current soil-vegetation-atmosphere transfer (SVAT) and numerical weather prediction (NWP) models use increasingly complex descriptions of the physical mechanisms governing land surface processes. They require large numbers of soil and land surface parameters controlling the vertical fluxes. Uncertainty in land surface parameterisation and the nature of landscape controls may lead to considerable uncertainty in predicted land surface fluxes and state variables such as soil moisture. There also remains significant uncertainty in the data used to calibrate such models and constrain the model's parameter set.

Determining the spatial and temporal variability in land surface processes over large areas and long time periods is a difficult task. This variability underlines the need for proper determination of the SVAT parameters used in the land surface parameterisation. Improved characterisation at larger landscape scales involves aggregation over heterogeneous surfaces. Such aggregation has frequently been approached in a lumped fashion, requiring single effective parameter values which would allow SVAT and NWP models to yield realistic regional-scale surface fluxes.

Stochastic methods have been developed which successfully reduce the uncertainty of the most important surface characteristics or SVAT parameters by comparing random model output to observed time series of remotely sensed variables. This approach acknowledges and is based on the inherent uncertainty of both SVAT model parameterisations and the actual measurement of thermal signatures of the land surface.

Various case studies have shown that the remote sensing in combination with SVAT modelling has significant potential in improving the estimation of land surface fluxes and derived variables. These studies focus on the use of satellite derived surface characteristics (land use) and on estimation of surface turbulent fluxes from RS data. Successful surface flux estimation has so far been limited to cases where the horizontal and spatial variability in surface temperature and reflectance is large and dominates the distribution of surface fluxes. As an example, we describe a recent algorithm for deriving surface fluxes and surface wetness from remotely sensed

surface temperatures and albedo which has been used successfully for soil moisture assimilation in a NWP model case study.

However, turbulent fluxes at the land surface and atmospheric boundary flow are controlled by factors which cannot be directly monitored from space platforms, in particular the aerodynamic properties of the land surface. For long term monitoring or estimation of surface fluxes, additional information on the aerodynamics is therefore crucial. For this, routine surface flux estimation is probably best achieved when combined with or embedded within a NWP analysis system. Following a review of several recent studies on the assimilation of satellite derived heating rates in regional atmospheric mesoscale models, we will discuss progress towards the use of a stochastic method to match measured and simulated surface temperature changes (heating rates) in order to obtain improved estimates of several key land surface parameters.

1. Introduction

Determining the spatial and temporal variability in land surface characteristics and processes over large areas and long time periods is a difficult task, and considerable effort has been put into gaining experience and deriving appropriate models to deal with this challenge. However, despite improvements in prediction of the surface energy balance through the use of remote sensing data, there remains the lack of appropriate measurements and prediction methods for surface fluxes and soil moisture over a range of space and time scales.

These difficulties are apparent in analyses of data collected during multidisciplinary experiments such as HAPEX or FIFE: whereas a certain level of accuracy of the surface fluxes was achieved using vegetation indices and thermal infrared measurements, little new insight was gained about subjects such as water redistribution at the regional scale or multi-scale water storage status and dynamics.

Various Soil-Vegetation-Atmosphere Transfer (SVAT) schemes have been developed for use with General Climate Models (GCMs) and Numerical Weather Prediction Models (NWPMs). However, SVAT models face various difficulties which include: (1) comparable complexity between system components; (2) scaling incongruities between atmospheric, hydrological and terrestrial components; and (3) validation of SVATs at appropriate space and time scales.

The need for improved characterisation of soil and land surface properties at regional and global scales is generally recognised. This involves aggregation over heterogeneous surfaces. SVATs approach land surface heterogeneity and subgrid variability either in a lumped fashion (with single effective, aggregated parameter values) or in the distributed fashion of a tile approach (with multiple optimised parameter sets or even multiple optimised sub-models, combined with the use of weighted averages).

Various schemes have been used for obtaining aggregated parameter values, including: (i) simple linear averaging weighted by fractional areas; (ii) weighted harmonic means; and (iii) logarithmic averaging. However, each scheme is

fundamentally reliant on accurate measurements which can not be achieved because of fine scale heterogeneities (Beven, 1995).

In this paper we first address the complexity of Soil Vegetation Atmosphere Transfer models and the uncertainty in prediction of land surface fluxes. Next we discuss the use of remote sensing with land surface schemes and in particular the conditioning of SVAT model parameters with remote sensing imagery and time series of remote sensing data. In the final section we discuss linking remote sensing, land surface schemes and numerical weather prediction models and we will briefly outline some recent progress.

2. Complexity of Soil Vegetation Atmosphere Transfer models and uncertainty in prediction of land surface fluxes

Current soil-vegetation-atmosphere transfer (SVAT) and numerical weather prediction (NWP) models include increasingly complex descriptions of the physical mechanisms governing land surface processes. The current trend in modelling surface fluxes seems to be towards even more complex SVAT structures which require large numbers of soil and land surface parameters controlling the vertical fluxes. The underlying rationale is that improved process representation will result in parameters which are easier to measure or estimate. However, this is not necessarily so, mainly because SVAT models require *effective* values for the various parameters at patch, regional or larger scales which are not easily estimated. Surface energy fluxes can vary significantly in space and time due to the variability in land surface properties. Recent studies have shown that characterising such properties is fraught with difficulties, as determining representative parameterisations is non-trivial due to our inability to accurately measure land surface properties.

Modelling of environmental systems may therefore lead to significant predictive uncertainty due to the complexity of the systems to be simulated. Uncertainty in land surface parameterisation and the nature of landscape controls may lead to considerable uncertainty in predicted land surface fluxes and state variables such as soil moisture.

Where *measurement* of relevant model parameters cannot be achieved, parameters may often be identified through *calibration* to measured fluxes. However, there remains significant uncertainty in the data used to calibrate such models and constrain its parameter set (Franks and Beven, 1997a). Often flux data used for calibration do not display the full range of possible system dynamics and hence the informative content of the data may be limited (Franks 1999). This will necessitate routine measurements of the land surface behaviour over longer time periods than are typically collected through intensive field campaigns such as FIFE, ABRACOS and HAPEX.

Increased complexity involves more parameters which may lead to increased uncertainty in prediction. On the other hand, simpler model structures may result in more robust parameter calibration but also potential uncertainty due to the simple model representation. SVAT models are typically over-parameterised with respect to the available calibration data and the complexity of the models provides non-unique optimal parameter sets.

Franks and Beven (1997ab) and Franks *et al.* (1997) describe a method for estimating the predictive uncertainty associated with possible parameterisations as applied to a simple SVAT model (TOPUP; see Beven and Quinn, 1994; Quinn *et al.*, 1995) forced with data sets from different climatic regimes. TOPUP is a SVAT model that represents the key physical processes controlling surface energy fluxes in a realistic but parametrically refined manner. This model incorporates the effects of near-surface stability conditions for the calculation of aerodynamic resistance. Unlike other more complex SVAT constructs, TOPUP-SVAT requires a minimum of only eight parameters to be specified.

The rationale for developing a simple model structure is that simplicity is necessary to empirically validate the use of such SVAT models in the field. Limited calibration data are available for such purposes, again highlighting the significant parametric and predictive uncertainty existing in the calibration and evaluation of SVAT models. This problem is compounded for more complex models that are grossly over-parameterised with respect to the available calibration/evaluation data sets.

Franks and Beven (1997a) and Franks *et al.* (1997) used the Generalised Likelihood Uncertainty Estimation (GLUE) methodology developed by Beven and Binley (1992) as a way of dealing with multiple acceptable parameter sets within a Bayesian Monte Carlo framework. The GLUE methodology involves the following steps. First, a large number of model runs are made with the simple SVAT model, each parameterised with random values of the parameters chosen from uniform distributions across the parameter ranges. Next, the acceptability of each run is assessed by some chosen likelihood measure calculated from comparison of observed and simulated responses. Following the rejection of non-behavioural runs, the likelihood weights of the retained runs are rescaled so that their cumulative total is 1.0. Finally, at each time step the predicted output from the retained runs are likelihood weighted and ranked to form a cumulative distribution of the output variable from which chosen quantiles can be selected to represent the model's uncertainty.

Franks and Beven (1997a) used TOPUP with meteorological data and evaporation measurements obtained during two intensive field campaigns of the ISLSCP Field Experiment (FIFE) and two periods of measurements in the UK-Brazilian ABRACOS project. They used 95% quantiles to determine the uncertainty bounds. The two parts of Figure 1 show that significant uncertainty is associated with the predictions of the latent heat flux, as indicated by the width of the estimated uncertainty envelope.

The uncertainty bounds for (top) IFC-3 and (bottom) IFC-4 were in each case conditioned on the data from those periods alone. These uncertainty bounds were calculated by using behavioural thresholds to retain the best 10% of the realisations for each of the data sets. Note that the figure displays very different behaviour between the two periods; IFC-3 contains a storm event followed by relatively high rates of evaporation whereas IFC-4 represents a very dry period. The estimated uncertainty envelope reaches about 0.5 mm/h in IFC-3 and about 0.1 mm/h in IFC-4. Note also that the uncertainty envelope does enclose the entire observed evaporation record for IFC-3 and for most days of IFC-4. There will be deficiencies in the model structure and/or the adequacy of the calibration data if the observed flux is not enclosed by the envelope.

Uncertainty estimates for the Amazonian pasture site using 1990 (top) and 1991 (bottom) data obtained in the ABRACOS experiment are shown in Figure 2 Uncertainty envelopes are typically between 0.05 and 0.25 mm/h.

Likelihood distributions of acceptable models may be derived by conditioning on one or more calibration periods. It is shown that there is considerable potential for constraining the uncertainty with additional data. It is shown that poor predictions may be due to calibrations based on insufficient or unrepresentative data. This is demonstrated in the next two figures.

Figure 3 shows 95% uncertainty estimates of the FIFE IFC-4 with the likelihoods conditioned on the IFC-3 period using a threshold to retain the best 10% of realisations. The figure displays wide uncertainty because many of the parameterisations which are acceptable with respect to IFC-3 are shown to be poor simulators for the IFC-4 period. The figure indicates that there is considerable potential for constraining the uncertainty with additional data.

Figure 4 shows the 95% uncertainty estimates for a section of 1991 ABRACOS data with the likelihoods having been conditioned on the 1990 period using a threshold to retain the best 10% of realisations. This figure displays wider uncertainty for 1991, due to over-conditioning on the particular circumstances that comprise the 1990 data set.

A reason why the uncertainty bounds do not do so well for 1991 when conditioned using the 1990 data may be because the 1990 data set is relative dry, whereas the 1991 data set is significantly wetter. This is also shown by Figure 5 which shows a scatter plot of the daytime evaporative fraction plotted against corresponding net radiation for the 1990 and 1991 ABRACOS grassland data sets. The lower evaporative fraction values attained in 1990 indicate generally drier conditions.

Parameter values determined by calibration must be considered as conditional values only: conditional on model structure, on the other parameter values used; and on the period of calibration. Availability of a wider range of data (or different types of data) may allow improved conditioning and elimination of a larger number of parameter sets (or model structures).

Using the same TOPUP model, as well as the same meteorological forcing data and evapotranspiration measurements (FIFE and ABRACOS), Franks *et al.* (1997) show the range of modelling efficiencies generated, where the efficiency measure used is the proportion of total variance explained (see Nash and Sutcliffe, 1970). The sensitivity of the SVAT model may then be illustrated by comparing cumulative distributions for discrete performance classes in terms of cumulative evapotranspiration or modelling efficiency. A total of 20,000 realisations were ranked according to the cumulative evapotranspiration totals (or the efficiency measure) into 10 groups of 2000 realisations. Cumulative distributions of parameter values were plotted for each parameter. A straight line would represent a uniform distribution of the parameter reflecting insensitivity for the performance range, whereas a marked departure from the straight line would represent a non-uniform distribution, indicating sensitivity and hence the relative importance of the parameter.

Figure 6 shows that the sensitivity of the parameters, when compared with the observed records of evapotranspiration through the efficiency measure, provides insight into the acceptability of the model structure. Good model efficiencies are achieved across the range of parameters considered. This implies that robust calibrations are not always achieved, resulting in *equifinality* of different parameter sets. The robustness of SVAT schemes in calibration would be improved by reducing the dimensionality of the parameterisation, either by fixing some of the parameters or reducing the complexity of SVAT constructs. It was considered that the problem of equifinality may be endemic to SVAT type models for land surface fluxes. Further constraining of such uncertainty will require additional measurements. This may be achieved by longer periods of calibration data which display as much of the natural system dynamics as possible, by the exclusion of additional parameter sets or through collection of additional data of different types, such as water table levels or soil moisture measurements. The use of remotely sensed thermal imagery for such a purpose is discussed in the next section.

3. The use of remote sensing with land surface schemes: conditioning of SVAT model parameters.

Numerous schemes and methodologies have been proposed to provide estimates of land surface fluxes utilising thermal signatures derived from a variety of remote sensing platforms. However, deriving estimates of heat fluxes from thermal signatures alone, in common with SVAT models, is subject to uncertainty. To derive an instantaneous heat flux estimate, land surface parameters must be specified. Additional uncertainty must be associated with such remote estimates due to the fact that thermal measurements are typically incommensurate with SVAT model variables and parameters (see Stewart *et al.*, 1998). Corrections must be applied to the raw radiance data to account for factors such as variable atmospheric effects, non-black body emissivity of the land surface, etc. As such, latent heat fluxes estimated in this way are subject to significant uncertainty through the requirement to parameterise the model which interprets the remote sensing.

Landsat TM data have been used by Franks and Beven (1997b) to represent the pixel-scale variability in land surface fluxes at the time of the overpass across the 15 km x 15 km FIFE domain in Kansas. Using a residual energy balance model (by which sensible heat transfer estimated from the surface/near-surface air temperature difference is subtracted from the available net-radiant energy) it is shown that substantial variability in latent hear flux (λE) may be predicted across the domain (Figure 7).

However substantial uncertainty is shown to be associated with the remote sensing derived "observations" of λE because they are based on an interpretative model with many approximate assumptions and uncertainty in various key parameters including: surface temperature, albedo, NDVI, surface roughness and wind speed. This uncertainty is estimated with a fuzzy measure approach. Multiple realisations of the TOPUP SVAT model were run over the longer time period of the third FIFE Intensive Field Campaign (IFC-3) with a large number of different sets of parameter values. These TOPUP model realisations were made with a wide enough range of parameters to represent the variability of fluxes across the domain. The authors' interest was in predicting *areally-averaged* landscape fluxes over the longer time period with the

requirement that cumulative values of these landscape fluxes based on TOPUP predictions were consistent with the *instantaneous* pixel estimates obtained from Landsat TM for the single time step. A fuzzy disaggregation technique is then described by which the spatial distribution of Landsat derived fluxes may be used to condition the parameter sets for the TOPUP modelling to reflect the (uncertain) flux estimates at the time of the image. Figure 8 shows the subsequent derived weighted mean and the 5% and 95% quantiles of the range of predictions in the landscape when the disaggregation model is driven with the areally averaged FIFE IFC-3 meteorological forcing data.

More recently Franks and Beven (1999) presented the results of an extension of the fuzzy disaggregation scheme to multiple Landsat imagery. They obtained areally-weighted latent heat fluxes according to the distributions of estimated fluxes derived from three separate Landsat TM overpasses (see Figure 9).

Various case studies have shown that the use of remote sensing in combination with SVAT modelling has significant potential in improving the estimation of land surface fluxes and derived variables. Successful remote measurement of fluxes or state variables may provide additional information with which to calibrate SVAT models. For example, Boulet (1999) has shown with a SVAT model (SVATsimple) based on the concept of potential infiltration/evaporation capacity how hydrodynamic soil parameters may be adjusted by minimising the difference between observed and simulated radiative surface temperatures.

Stochastic methods have been developed which successfully reduce the uncertainty of the most important surface characteristics or SVAT parameters by comparing random model output to observed time series of remotely sensed variables. This approach acknowledges and is based on the inherent uncertainty of both SVAT model parameterisations and the actual measurement of thermal signatures of the land surface.

McCabe *et al.* (1999) adapted the TOPUP-SVAT model to show how a time series of thermal data collected over a dry-down period can be used to provide improved model parameterisation. Their TOPUP adaptation generated surface temperature (T_s) values by solving the full set of equations for the energy balance and the aerodynamic and plant canopy components of sensible heat and latent heat transfer (see Franks, 1999). They used combinations of feasible land surface characteristics associated with broadly defined vegetation types to parameterise the SVAT model. Uncertain parameter correlation was permitted which coupled individual model parameters to simplified functions of the canopy height. Three classes of land surface cover were distinguished: bare soil (sand), grass and trees. Parameter ranges for each of the variables of interest can be defined *a priori* based on physical relations, from experience or published literature.

Table 1 shows the distinct ranges of feasible parameter classes that have been assigned in this study to the different land surface/vegetation cover types. In order to investigate the thermal and evaporative response to these broad parameterisations of a simple SVAT model, multiple parameter realisations are required. To sample the 'likely' parameter space for each identified land surface cover type, 5000 individual parameter sets were constructed. The randomly selected values for the individual

parameters are then forwarded into the model as *a complete parameter set*. For each sampled parameter set, TOPUP was initialised with a fully wetted root zone, i.e. for unstressed conditions.

The adapted TOPUP was then run with a long period of rainfall-free forcing data derived from the UK-Brazilian ABRACOS campaign in Amazonia, to investigate the dry-down behaviour of the various surface covers in terms of surface energy fluxes and thermal signatures. The model was run for each of the 5000 parameter sets over 1700 hourly time steps. In addition, a single parameter set was selected for each cover type from within the feasible ranges of the cover-specific parameter space. These unique parameter sets were then used to parameterise TOPUP-SVAT and were subsequently employed as *pseudo-observation records* for the associated surface cover. The temporal response of the temperature series derived from these pseudo observations was designated as the *'true' surface response* (as would have been obtained with remote sensing) against which the model predictions could be compared.

Figure 10 shows a plot of the modelled range of latent heat flux against the aerodynamic surface temperature calculated by TOPUP during the initial *unstressed conditions*, extracted at the beginning of each of the 1700 runs. A distinct structure between the defined land covers can be observed. As expected, the bare soil displays the highest measures of instantaneous surface temperatures, whereas the tree class shows the lowest instantaneous temperatures and a wide range of latent heat fluxes. The plot illustrates the relative uncertainty in estimating latent heat fluxes as a direct function of remotely sensed radiative surface temperatures: if one could accurately measure an appropriate aerodynamic surface temperature, the effect of parameter uncertainty is such that a large range of inferred latent heat fluxes is possible. It is therefore clear that parameter uncertainty prohibits the retrieval of instantaneous fluxes from surface temperature measures alone.

Surface temperatures are significantly sensitive to the aerodynamic surface properties. However, a recent sensitivity analysis of TOPUP indicated that latent heat fluxes are relatively insensitive to aerodynamic properties given uncertainty in the other model parameter values (Franks *et al.*, 1997). Additionally, model predicted aerodynamic surface temperature is not the same as the remotely measured radiometric surface temperature. The relation between the aerodynamic and radiative surface temperatures may be expressed as a function of the Leaf Area Index (Chehbouni *et al.*, 1997 in Boulet, 1999 p. 95), although the difference between the two is approximately constant over the typical range of temperatures (Huband and Monteith, 1986).

In terms of land surface flux behaviour in a drying period, differences in unstressed fluxes might be of secondary importance. Of more significance is the accurate simulation of how and when a surface reduces and stops evaporative losses, as this is more directly linked to the total available moisture store of the land surface. It is therefore expected that the *temporal pattern* of energy flux response will provide greater insight into the *functional behaviour* and appropriate parameter values than any single estimate of the instantaneous flux is capable of doing. By comparing the temporal pattern of thermal responses, one may therefore achieve robust characterisation of the land surface function as well as a degree of parameter tractability.

Equifinality means the existence of non-unique parameters, however it also means that multiple parameter sets produce the same *function*. So one should attempt to measure the function. The parameters are then only of secondary importance as long as the parameter set produces the correct function. From a modelling point of view we do not strictly need the optimal data set if we can measure and reproduce the function of the land surface.

McCabe *et al.* (1999) aimed to identify the *functional behaviour* of the land surface in terms of latent heat fluxes, through reference to the temporal changes of the surface thermal signature. To achieve this, they normalised the 'contending modelled thermal responses' relative to the observed (sensed) thermal sequence. The modelled thermal responses were scaled to the extreme temperatures of the 'observed' record, such that the modelled response matches the observed record at the positions of maximum and minimum temperature. The remaining temperatures are then fitted accordingly, using a simple linear equation to adjust values throughout the temporal series. Next, the 'contending' model parameter sets were evaluated with respect to the 'matching' to the observed sequence through an objective function based on sum of squared errors. The best 1% of model simulations (50 out of 5000) that reproduced the normalised temporal patterns of surface temperature were retained as 'acceptable' simulators of the (pseudo-) observed data. The retained acceptable parameter sets were then analysed in terms of the range of cumulative latent heat fluxes, the time series of latent fluxes, and their constituent individual parameter values. This was achieved for both grass and tree land surface cover types.

As an example, Figure 11 shows cumulative likelihood plots for the pre- and post-conditioned randomly sampled parameter sets for grass and for trees. The solid line refers to the pre-conditioned (5000) parameter sets, whilst the dashed lines represent the cumulative likelihood of the (50 or 1%) parameter sets deemed acceptable after comparison to the 'observed' thermal time series. These plots show the effect of the conditioning with respect to the relative constraint of two of the model parameters (available soil moisture storage SRMAX and minimum surface resistance RSMIN), and the cumulative latent heat flux over the period of simulation.

Figure 12 shows the 95% uncertainty bounds of latent heat fluxes for the grass land-surface cover type. The solid lines refer to the upper and lower bounds of the latent heat fluxes of the 5000 random samples from the grass cover parameter ranges across the 1700 time-steps. As can be seen, large uncertainty must be associated with the predicted fluxes following the specification of any set of unique parameter values for this cover type.

The dashed lines, however, represent the resultant predictive uncertainty following the conditioning of the parameter sets on the normalised temporal sequence of surface temperatures. As can be seen, the uncertainty envelope is drastically reduced relative to the un-conditioned parameterisations. It can be seen that at time step 430 (solid line), some realisations of the parameter space produce an ET flux of zero, indicating that the soil moisture store in the grass is at a minimum and that the surface exhibits conditions representative of a "dry" state. This situation is protracted for the normalised prediction (dashed line) which produces "dry" conditions at time step 1030. This indicates that whilst gross uncertainty in instantaneous fluxes must be

expected when inferred from a thermal measurement alone, a temporal series may be usefully employed in constraining this uncertainty. Additionally, the conditioned realisations are observed to cease evaporating at time step 1255 while the unconditioned response continues beyond the 1700th time step. The time required for the conditioned realisations to cease evaporating (in this case approximately 200 hours) may provide a means of examining the period within which the surface response changes from atmosphere controlled to moisture limited evaporation.

This assessment led to the following conclusions. The prediction of latent heat fluxes from absolute measures of surface temperatures (see Figure 10) was seen to be inherently uncertain. Through the analysis of a temporal series of latent heat fluxes, an enhanced prediction of the dry-down dynamics could be achieved. Additionally, the narrowing of the uncertainty bounds for the normalised temporal pattern allowed an improved parameterisation of SVAT constructs to be achieved. This is important because SVAT models are generally over-parameterised with respect to the available data.

The simple linear normalisation process that was employed, allowed the problem of correlating 'sensed' radiative temperatures and modelled aerodynamic temperatures to be addressed. Acknowledging that the difference between aerodynamic surface temperature and sensed radiative temperature is functionally similar, the implementation of a methodology that discriminates between parameter sets based on their temporal similarity to the observed temperature record will more closely reproduce that observed response.

It is expected that the use of temporal patterns may provide the greatest insight when these patterns cover a period of wetting-up/drying-down dynamics. The importance of capturing this period from an unstressed to a stressed state is that it allows direct examination of vegetation response and the associated behavioural changes, thus facilitating a refinement of parameter specification. Such use of a time series of aerodynamic surface temperatures may reveal appreciable insight into the dynamics of the dry-down phase over a variety of simulated surface covers. Inter-class parameter behaviour may provide some useful insights into the controlling or more sensitive parameters in the SVAT model. It is shown that the implementation of a conceptually simple normalising procedure and the associated recognition of multiple parameter set or non-unique solutions can facilitate an improved and tightly constrained range of predictions for many of the model parameters.

Following the above results of McCabe *et al.* (1999), the question remains to what degree T_s *measurements* can produce inferences into the functional behaviour of the land surface fluxes. Work is currently in progress to apply the methodology outlined here to long-term field obtained in a SE Australian catchment study. However, this will require more rigorous investigation into appropriate likelihood functions to remove issues of subjectivity.

4. Linking remote sensing, land surface schemes and numerical weather prediction models

As discussed in the previous section, significant uncertainty must be associated with the specification of all surface and sub-surface parameters. This uncertainty is already

marked at the local patch (or plot) scale, and must be even greater when spatial variability of these parameters is considered. Whilst aerodynamic properties cannot be assigned without uncertainty, a degree of characterisation may be achieved through the specification of coarsely defined, uncertain ranges for each broad class of surface type. Additionally, a degree of uncertain correlation between parameters must also be expected – available moisture must be a function of rooting depth, which will in some manner be uncertainly linked to the vegetation height.

Current land surface schemes such as BATS and SiB have complex data requirements. This frequently leads to a combination of sources to gather all the required data. Menenti (1998) refers to the work of Harding *et al.* (1996) who presented a simulation study in HAPEX-Sahel with a Mesoscale Meteorological Model in which the required data were obtained from satellite measurements, surface measurements and land surface models, as well as values published in the literature. International Field Experiments such as MONSOON-90, EFEDA, HEIFE and HAPEX-Sahel have seen significant usage of a wide range of satellite and airborne sensor systems providing observables, such as surface temperature, surface hemispherical reflectance, spectral vegetation index, aerodynamic roughness length, leaf area index, backscatter coefficient and microwave emissivity (Menenti, 1998).

Remotely sensed variables can be used in land surface parameterisation in two ways. First, land surface characteristics, such as vegetation coverage, leaf area index or amount of high vegetation are usually prescribed fields in NWP and climate models. New satellite derived land use products have become available that allow for a more detailed description of the land surface characteristics, both in temporal and in spatial resolution (e.g. USGS, 1997). These products are being incorporated in NWP and climate models (e.g. Hagemann *et al.*, 1999). Second, temporal and spatial patterns of surface temperature and shortwave reflectance are interpreted in terms of surface turbulent fluxes, which can be used to control prognostic surface variables in NWP models (e.g. van den Hurk *et al.*, 1997). Both issues are addressed in example studies below.

4.1 Impact of a change of land surface characteristics on surface energy balance calculations in a NWP model.

The impact of modifying the land surface characteristics on a NWP forecast cycle was examined by van den Hurk *et al.* (1999). Preliminary results of this study are shown below.

Two series of runs with the regional climate model RACMO (Christensen and van Meijgaard, 1992) with varying land surface characteristics for the European area in the period March – November 1995 were executed. In one series, the land surface characteristics LAI, vegetation coverage, vegetation roughness and surface albedo were derived from the ECHAM4 climate database (Claussen *et al.*, 1994) and kept constant throughout the season. In the second series, these surface characteristics were derived from the USGS (1997) 1 x 1 km NOAA based land use database. For each of the 18 prescribed land surface types in this database, seasonal cycles of LAI, vegetation coverage, vegetation roughness and surface albedo were prescribed. In both series of RACMO runs, sea surface temperatures and lateral boundaries were taken from ECMWF analysis products.

To evaluate the impact of incorporating seasonal changes in the land surface characteristics, the average forecast score of near-surface temperature and relative humidity was calculated for all European synops stations, using operational synops data. Figures 13-16 show the resulting average biases and rms-values for both 2m temperature and 2m relative humidity (RH).

It may be observed that the temperature bias, i.e. the difference between predicted and observed temperatures, is hardly affected by the new land use characterisation. On the other hand, there is a slight bias reduction and improvement in the rms for relative humidity values when the new land surface climatology is used. The bias reduction in RH is most apparent early in the growing season, where the old vegetation database prescribes higher amounts of vegetation than the new one, resulting in larger overestimation of the surface evaporation and RH. The reduction in rms of RH is most apparent in the summer season, when the forcing by the lateral boundaries is weaker owing to a less dominant zonal flow pattern.

These results imply that the improved resolution in land use cover does result in a slightly improved spatial representation of critical land surface characteristics. The results, however, show only a moderate impact of the prescribed land surface characteristics, which is most likely due to the fact that the climate of Europe is strongly controlled by the North Atlantic. It is very likely that stratification of the results shown here into continental and sea coastal synops stations would reveal a larger sensitivity of the forecast scores to prescribed land surface characteristics.

4.2 Remotely sensed spatial and temporal variability of surface characteristics for updating surface fluxes in NWP

Spatial and temporal variability of observed surface temperature may be used to assess the (variability) in surface evaporation conditions. The surface energy balance at sites with high surface temperature heating rates in a diurnal cycle can be assumed to be governed by sensible heat exchange, while low heating rates indicate areas where surface cooling takes place by evaporation (McNider *et al.*, 1994). Jones *et al.* (1998a) use GOES derived surface temperature changes in time to update the soil moisture condition in a regional atmospheric model. They adjusted the soil moisture content in the model to a value which forced the model to exhibit a surface heating rate comparable to the satellite observations.

In a case study (Jones *et al.*, 1998b), it is shown that the method is able to pick up a soil moisture distribution which is compatible with a record of antecedent rainfall in the US Great Plains area. Figure 17 shows the 24 hrs accumulated rainfall for 7 and 8 September 1991, while in Figure 18 West-East transects of the average surface soil moisture content for a uniformly initialized control run and an experimental assimilation run are displayed. The experimental run shows a clear increase in soil moisture content in the Eastern part of the domain. The West-East gradient of surface wetness was confirmed by a microwave surface emittance image from SSM/I (figure not shown).

At the Royal Netherlands Meteorological Institute (KNMI) preliminary results of this heating rate method have recently become available. Diurnal surface temperature

changes derived from METEOSAT images of the area encompassing The Netherlands, Belgium and a small portion of the UK in various periods in 1995 have been compared to RACMO estimates of the surface temperature change. Heating rates are computed as $(T_{max}-T_{min})/(t_{max}-t_{min})$ where T= temperature and t=time, with 0600 UTC$<t_{min}<$1100 UTC and 1200 UTC$<t_{max}<$1600 UTC.

Figure 19 summarises some early results obtained in this work. Shown are the differences between RACMO and METEOSAT heating rates for 25 June 1995 for 7 synops stations in this area. These stations were selected on basis of the absence of clouds during most of that day, enabling a more straightforward interpretation of satellite derived heating rates. The RACMO heating rates were calculated for two separate RACMO runs: one with a relatively dry soil moisture content, and one with a 5% wetter soil. Results of these two runs are interconnected with lines for each individual synops station. Plotted is the difference between the RACMO and METEOSAT heating rates versus the error in relative humidity calculated by RACMO, compared to the synops observation. It is clearly seen that (a) wetter soil moisture inititialization reduces the error in RH and reduces the surface temperature diurnal cycle, and (b) the slope of this sensitivity points at a minimum error in RH for heating rates which are very similar to the heating rate derived from METEOSAT observations. The important message from this simple graph is that the information content in the METEOSAT surface temperature change is compatible to the information in the synops data. Cloud screening and further examination for other areas and seasons are ongoing research topics.

In contrast to the heating rate method explored above, the SEBAL (Surface Energy BAlance for Land)-algorithm estimates land surface fluxes from the *spatial variability* of remotely sensed surface temperature and reflectance as observed in individual scenes.

SEBAL (Bastiaanssen, 1995; Bastiaanssen *et al.*, 1998a) is a land surface energy balance algorithm for use with remotely sensed surface temperature, surface reflectivity and Normalised Difference Vegetation Index (NDVI) data. The scheme represents a one-layer resistance transfer scheme which derives surface resistance, sensible heat (H) and latent heat (λE) fluxes and near-surface soil moisture. It has been used over a range of spatial scales (10 m -5 km) and temporal scales (30 minutes -16 days). The SEBAL scheme combines a certain degree of empiricism with explicit use of the *spatial variability* in surface temperature and surface albedo across cloudfree scenes. Other parameters are assumed to be constant in the domain of operation. SEBAL requires few if any concurrent field observations. Downward shortwave and longwave radiation components are computed using a given constant atmospheric transmissivity, and an empirical function of air temperature, respectively. The soil heat flux (G) is calculated as a fraction of net radiation (Q*) depending on (among others) NDVI.

The sensible heat flux H is calculated in a series of steps. The first step is to make a scatter plot for the entire image of surface albedo versus surface temperature T_s. Assuming that the scene contains very wet and very dry pixels, the pixels with large evaporation rates may be recognized as having low temperatures and low albedos, whereas areas with little or no evaporation show high surface temperatures and high albedos. Scatter plots obtained for large heterogeneous regions frequently show an

ascending branch controlled by moisture availability and evaporation, and a radiation-controlled descending branch where evaporation is negligible. If the radiation-controlled descending branch is well-defined, the aerodynamic resistance for dry land surface elements may be estimated reasonably well.

Next, the relationship between surface temperature T_s and near-surface temperature gradient ΔT is assumed to be quasi-linear. Two extremes are identified for the image: a wet extreme where $\lambda E >> H$ and $\Delta T=0$, and a dry extreme where $\lambda E=0$. These extremes are used as anchors for the quasi-linear relationship relating ΔT to T_s. This relationship allows ΔT to be estimated for any T_s across the image.

Finally, through the use of local surface roughness (z_0), based on the NDVI and the assumption of a fixed z_{0M}/z_{0H} ratio, together with a set of flux profile relationships for temperature and momentum, the sensible heat flux may thus be calculated for every pixel. λE is then the residual term in the energy balance equation.

Such a λE map shows the spatial variability in the latent heat flux based on one specific image. SEBAL output may also include isolines of the evaporative fraction $\Lambda = \lambda E/(H+ \lambda E) = \lambda E/(Q^*-G)$ which is a convenient surface wetness parameter because it has been shown to remain fairly constant from mid morning through to mid afternoon (see Shuttleworth *et al.*, 1989; Bastiaanssen *et al.*, 1996)

The SEBAL scheme (which is based on employing the observed *spatial variability* in surface albedo and surface temperatures as observed in individual scenes) has been used in a wide range of case studies and has been compared with ground measurements in different environments. In the EFEDA project SEBAL was used with imagery obtained with NS001 research aircraft imagery as well as Landsat TM, NOAA-AVHRR and METEOSAT satellite data and its predictions compared with groundbased flux measurements and soil moisture observations (see Bastiaanssen *et al.*, 1996; Menenti and Bastiaanssen, 1997; Bastiaanssen *et al.*, 1997; and Bastiaanssen *et al.*, 1998b. Bastiaanssen *et al.* (1996) used NASA C-130 NS001 radiometer data as well as hourly METEOSAT images to carry out a multi-resolution study and intercomparison of flux predictions over three EFEDA supersites in Central Spain. They describe a technique to derive area-effective bulk surface resistance and Priestley-Taylor α parameter estimates using SEBAL in association with a set of aggregation rules. This technique can be used to validate the large area surface resistance and evaporation predicted by mesoscale SVAT models and other Manabe type bucket land surface models.

In a recent paper Bastiaanssen *et al.* (1998b) compared surface fluxes predicted with SEBAL with data obtained in large-scale field experiments in Spain (EFEDA), Niger (Hapex-Sahel) and China (HEIFE). The validation procedures tested in their study included turbulent surface fluxes measured in the field; airborne turbulent measurements; and soil moisture profiles measured in the field. In addition SEBAL results were also compared in Qattara Depression and the Nile Delta in Egypt with the output of hydrological models. These validations may be summarised by noting that the accuracy of SEBAL evaporation results varies with the scale of the validation. Bastiaanssen *et al.* (1998b) indicate that SEBAL accuracy is 81% when compared with groundwater modelling results, 92-95% when compared with the output of

surface hydrology models, about 90% for soil moisture measurements, 85-95 % for surface flux measurements with towers and finally 99% when compared with airborne flux measurements.

An important drawback of SEBAL is its empiricism with respect to aerodynamic coupling between the land surface and the atmosphere. Information on aerodynamic exchange processes cannot be derived directly from remote sensing data. To overcome this problem, information from, for instance, a routine NWP data assimilation analysis cycle would probably constitute a significant addition when routine surface flux estimation is required.

Van den Hurk *et al.* (1997) described how evaporation maps derived from satellite data with the SEBAL land surface scheme may be used to assimilate (initial) soil moisture fields for use in an operational NWP model. They used SEBAL estimates of the evaporative fraction $\Lambda = \lambda E/(\lambda E + H)$, derived from the spatial patterns in surface temperature and albedo present in METEOSAT and NOAA-AVHRR imagery for the Iberian peninsula in the first week of July 1994 for soil moisture assimilation in RACMO. The evaporative fraction (which is fairly constant during the day, as pointed out earlier) derived by SEBAL was used to adjust the Λ value used in RACMO. This was achieved by adjusting the climatological background soil moisture content ω_b to a value of ω which minimises $\Delta\Lambda = \Lambda$ (RACMO) - Λ (SEBAL). Van den Hurk *et al.* (1997) carried out a series of runs with RACMO to obtain a relationship between ω and Λ.

Two sequences of RACMO runs were started from a similar soil moisture field for 1 July, generated by forcing RACMO to calculate evaporative fractions close to those simulated by SEBAL. In the control sequence no further adjustment of soil moisture was carried out. In the other experimental run, soil moisture was also adjusted using two later SEBAL estimates.

Figure 20 shows results of temperature and specific humidity bias of the two run sequences. The experimental run successfully avoids the positive temperature bias shown in the control run and also produces smaller bias in the specific humidity. Thus good results were obtained with SEBAL, although the range of soil moisture conditions encountered was somewhat limited. These results imply that satellite based information on the *spatial* variability of surface temperature (and shortwave reflectance) may be used in partitioning the available net radiant energy (Q*) into latent (λE) and sensible heat (H) fluxes from the surface.

It is obvious that there is a need to investigate if the above assimilation procedure works well for the full range of environmental conditions. This is currently explored using NOAA/AVHRR data for the whole of Europe and for all of 1995. The first results show that the remote sensing data contain a signal which is comparable with synops data when operated on a European scale (see van den Hurk *et al.*, 1998).

Su *et al.* (1998) note that the quality of the initialisation data and the data assimilation procedure determine the prediction skill of a NWP model. Their paper addresses the linkage between SEBAL, NOAA/AVHRR imagery and the RACMO NWP model for continental studies of land surface characteristics and surface fluxes over Europe and Africa. The links described by Su *et al.* (1998) include: (1) comparison between

RACMO predicted cloudcover and satellite imagery; (2) deriving land surface temperatures of brightness temperatures in Bands 4 and 5 of NOAA AVHRR by atmospheric correction using RACMO generated atmospheric water content; (3) characterisation of vegetation cover and land use using remote sensing data and DEM; (4) computation of incoming global radiation, albedo, NDVI, land surface emissivity, and surface roughness using geographic parameters, remote sensing data, DEM and RACMO derived optical properties of the atmosphere; (5) partitioning of the available energy into latent and sensible heat using the improved SEBAL algorithm and RACMO's regional potential air temperature at blending height; and (6) initialisation and updating RACMO using the SEBAL generated evaporative fraction.

5. Future work

As has been illustrated in previous sections, significant progress has been made in the use of remote sensing for improvement of (operational) land surface parameterisation. Several approaches are explored simultaneously: a better description of ("static") land surface characteristics such as vegetation parameters, a quantification of the uncertainties in SVAT model parameters guided by remotely sensed variability in time and space, and assimilation of prognostic quantities related to the availability of soil water for evaporation in NWP models.

Probably the most rapid progress is be expected in areas where various disciplines are brought into a common framework, thereby using the maximum information content from each of the disciplines. Shuttleworth (1998) rightly points at a hierarchy of parameters and variables that control the evaporation from the land surface:

- The amount of available radiative energy: this requires proper estimation of cloud cover, surface albedo and longwave radiation components
- The type of surface: this requires detailed mapping of the presence (and type) of vegetation
- The presence of water that can be evaporated: information on this quantity is probably best contained in (remotely sensed) surface temperature variability, both in time and in space, in combination with information on the aerodynamic properties of the surface and the flow.

A combination of data sources containing appropriate information content on each of these items will therefore yield optimal results.

Although an important issue, assimilation of cloud cover and radiation data has not been addressed explicitly in this paper. The other items are all covered in the demonstration studies described above.

Combining the issues addressed in this paper we can anticipate certain developments to occur in the near-future. First, further use of satellite derived surface characterisation products will be inevitable. In parallel to this, climate models (and maybe also NWP models) will invest in a more dynamic description of the vegetation, either by directly using on-line satellite information (such as spectral indices and albedo values), or by coupling the GCMs to interactive vegetation models, allowing for a two-way coupling between vegetation and climate.

Second, heating rates from geostationary satellite platforms seem to contain a useful amount of information on the bulk surface flux properties of a NWP or climate model grid box at fairly course resolutions. A further exploration of this information is foreseen at several climate and NWP research institutes. For the present, however, these bulk properties can only be applied in regions and periods where available radiation and soil moisture control the surface energy balance. Sensitivity to the parameterisation of aerodynamic characteristics is particularly obvious. In the assimilation schemes in the NWP-systems, equifinality of sets of model parameters *and* prognostic variables will be a difficult problem to handle. Therefore, applied research is needed in order to benefit from the stochastic approaches discussed in the first few sections. Repeated assimilation of remotely sensed variables, in combination with a stochastic modelling framework, will hopefully lead to achieving the general aim of representing the function of the land surface through enhanced large-scale remote sensing measurement techniques that explicitly recognise and incorporate the uncertainty associated with their derivation.

6. References

Bastiaanssen, W. G. M. (1995). Regionalisation of surface flux densities and soil moisture indicators in composite terrain. PhD Thesis, Wageningen Agricultural University, 288 pp.

Bastiaanssen, W. G. M., Menenti, M., Feddes, R. A. and Holtslag, A. A. M (1998a). A remote sensing surface energy balance algorithm for land. I. Formulation. J. Hydrol. 212/213, 198-212.

Bastiaanssen, W. G. M., Pelgrum, H., Droogers, P., de Bruin, H. A. R., and Menenti, M. (1997). Area-average estimates of evaporation, wetness indicators and top soil moisture during two golden days in EFEDA. Agric. Forest Meteorol. 87, 119-137.

Bastiaanssen, W. G. M., Pelgrum, H., Menenti, M., and Feddes, R. A. (1996). Estimation of surface resistance and Priestley-Taylor α estimates at different scales. In: J. B. Stewart *et al.* (eds.) Scaling up in hydrology using remote sensing. J. Wiley and Sons, Chichester, England, 93-111.

Bastiaanssen, W. G. M., Pelgrum, H., Wang, J., Ma, Y., Moreno, J. F., Roerink, G. J. and Wal, T. van der (1998). A remote sensing surface energy balance algorithm for land (SEBAL. 2. Validation. J. Hydrol. 212/213, 213-229.

Beven, K. J. (1995). Linking parameters across scales: Subgrid parameterisations and scale dependent hydrological models. Hydrol. Processes 9, 507-525.

Beven, K. J. and Binley, A. M. (1992). The future of distributed models: model calibration and uncertainty prediction. Hydrol. Processes 6, 279-298.

Beven, K. J. and Quinn, P. F. (1994). Similarity and scale effects in the water balance of heterogeneous areas, Proc. AGMET conference on The Balance of Water – Present and Future, AGMET, Dublin. September, 1994.

Boulet, G. (1999). Modelisation des changements d'echelle et prise en compte des heterogeneites de surface et de leur variabilite spatiale dans les interactions sol-vegetation-atmosphere. These pour obtenir le grade de Docteur de l'Universite Grenoble I. Grenoble, France (328 pp).

Chehbouni A., Lo Seen, D. L., Njoku, E. G., Lhomme, J. P., Monteny, B. and Kerr, Y. (1997). Estimation of sensible heat flux over sparsely vegetated surfaces. J. Hydrol. 188/189, 855-868.

Christensen, J. H. and Meijgaard, E. van (1992). On the construction of a regional atmospheric climate model. KNMI Scientific Report No. 147, 22 pp.

Claussen, M., Lohmann, U., Roeckner, E. and Schulzwerda, U. (1994). A global data set of land-surface parameters; Max-Planck Inst. f. Meteorologie, Rept. No 135, 23 pp.

Franks, S. W. (1998). An evaluation of single and multiple objective SVAT model conditioning schemes: Parametric, predictive and extrapolative uncertainty. Dept. of Civil, Surveying and Environmental Engineering, Research report 167.09.1998, Univbersity of Newcastle, Australia.

Franks, S. W. (1999). Extrapolative testing of a multi-objective conditioned SVAT model within an uncertainty framework (submitted for publication).

Franks, S. W. and Beven, K. J. (1997a). Bayesian estimation of uncertainty in land surface-atmosphere flux predictions, J. Geophys. Res.102, D20, 23, 991-23, 999.

Franks, S. W. and Beven, K. J (1997b). Estimating evapotranspiration at the landscape scale: A fuzzy disaggregation approach, Water Resour. Res. 33(12), 2929-2938.

Franks, S.W., and Beven, K. J. (1999). Conditioning a multiple patch SVAT model using uncertain space-time estimates of surface fluxes as inferred from remotely-sensed data. Water Resour. Res., submitted.

Franks, S. W., Beven, K. J., Quinn, P. F. and Wright, I. R. (1997). On the sensitivity of Soil-Vegetation-Atmosphere-Transfer (SVAT) schemes: equifinality and the problem of robust calibration, Agric. For. Meteorol., 86, 63-75.

Hagemann, S., Botzet, M., Dumenil, L., and Machenauer, B. (1999). Derivation of global GCM boundary conditions from 1km land use satellite data. Max-Planck Inst. f. Meteorologie, Rept. No 289, 34 pp.

Harding, R. J., Taylor, C. M. and Finch, J. W. (1996). Areal average surface fluxes from mesoscale meteorological models: the application of remote sensing. In: J. B. Stewart *et al.* (Eds). Scaling up in hydrology using remote sensing. J. Wiley and Sons, Chichester, England, pp. 59-76.

Huband, N. D. S. and Monteith, J. L. (1986). Radiative surface temperature and energy balance of a wheat canopy. 1. Comparison of radiative and aerodynamic canopy temperature, Boundary Layer Meteorol. 36, 1-17.

Hurk, B. J. J. M. van den, Meijgaard, E. van and Holtslag, A. A. M. (1999). A comparison of a regional daily forecast cycle and a regional climate simulation; EGS presentation, The Hague, 1999.

Hurk, B. J. J. M. van den, Bastiaanssen, W. G. M., Pelgrum, H., and Meijgaard, E. van (1997). A new methodology for assimilation of initial soil moisture fields in weather prediction models using METEOSAT and NOAA data. J. Appl. Meteorol. 36, 1271-1283.

Hurk, B. J. J. M. van den, Meijgaard, E. van, Su, Z. and Holtslag, A. A. M. (1998). Soil moisture assimilation over Europe using satellite derived surface fluxes. Paper presented at 2nd Conf. on BALTEX, Island of Ruegen, 25-29 May 1998.

Jones, A. S., Guch, I. C. and VonderHaar, T. H. (1998a). Data assimilation of satelloite derived heating rates as proxy surface wetness data into a regional atmospheric mesoscale model. Part I: Methodology. Monthly Weather Review 126, 634-645.

Jones, A. S., Guch, I. C. and VonderHaar, T. H. (1998b). Data assimilation of satellite derived heating rates as proxy surface wetness data into a regional atmospheric mesoscale model. Part II: Case Study. Monthly Weather Review 126, 646-667.

McCabe, M. F., Franks, S. W. and Kalma, J. D. (1999). On the estimation of land surface evapotranspiration: Parameter inference in SVAT modelling using a temporal record of thermal data. In: Proceed. 25th Hydrology and Water Resources Symposium Water 99, Brisbane, July 1999 (in press).

McNider, R.T., Song, A.J., Casey, D. M., Wetzel, P. J. , Crosson, W. L. and Rabin, R. M. (1994). Toward a dynamic -thermodynamic assimilation of satellite surface temperature in numerical atmospheric models. Monthly Weather Rev. 122, 2784-2803.

Menenti, M. (1998). Assimilation of multispectral measurements in interactive land surface models. Adv. Space Res. 22 (5), 611-624.

Menenti, M. and Bastiaanssen, W. G. M. (1997). Mesoscale climate hydrology: Earth Observation System-Definition Phase. Project NRSP-2-95-15. Beleids Commissie Remote Sensing, Delft, Netherlands, 197 pp.

Nash, J. E. and Sutcliffe, J. V. (1970). River flow forecasting through conceptual models. 1. A discussion of principles. J. Hydrol. 10, 282-290.

Quinn, P. F., Beven, K. J. and Culf, A. (1995). The introduction of macroscale hydrological complexity into land surface-atmosphere transfer models and the effect on planetary boundary layer development. J. Hydrol. 166, 3-4, 421-444.

Shuttleworth, W. J. , Gurney, R. J., Hsu, A. Y. and Ormsby, J. P. (1989). FIFE: The variation in energy partitioning at surface flux sites. Remote Sensing and Large-Scale Global Processes. Proceed. Baltimore Symp., IAHS Publ. 186, 67-74.

Shuttleworth, W. J. (1998). Combining remotely sensed data using aggregation algorithms; Hydr. And Earth System Sci. 2, 149-158.

Stewart, J. B., Engman, E. T. , Feddes, R. A., and Kerr, Y. H. (1998). Scaling up in hydrology using remote sensing: summary of a Workshop. Int. J. Remote Sensing 19(1), 181-194.

Su, Z., Menenti, M., Pelgrum, H., van den Hurk, B. J. J. M., and Bastiaanssen, W. G. M. (1998). Remote sensing of land surface fluxes for updating numerical weather prediction. Paper presented at EARSeL Symposium: Operational Remote Sensing for Sustainable Development, Enschede, Netherlands, 11-15 May 1998, 10 pp.

United States Geological Survey (1997). Global land cover characteristics database (http://uecwww.cr.usgs.gov/landdaac/glcc/globe_int.html).

LIST OF FIGURES

Figure 9
ISLSCP-FIFE grid areal latent heat fluxes derived through application of the fuzzy disaggregation scheme. The functional classes (each with similar SVAT behaviour) are areally weighted according to the distributions of estimated fluxes from three Landsat TM overpasses. (from Franks and Beven, 1999).

Figure 10
Aerodynamic surface temperature against latent heat flux estimates for unstressed conditions. Ranges are the result of 5000 randomly generated parameter sets produced for each class type. (taken from McCabe *et al.*,1999).

Figure 11
Cumulative likelihood plots of relevant parameters for both grass (a) and trees (b) (taken from McCabe *et al.*,1999).

Figure 12
Temporal pattern of latent heat flux for grass over model duration of 1700 time steps. Figure shows both pre (dashed) and post (solid)-conditioned model runs with 95% uncertainty limits (taken from McCabe *et al.*,1999).

Figure 13
Bias (predicted-observed air temperature) as obtained with RACMO for all European synops stations with the old ECHAM4 climate data base (dashed lines) and with the new NOAA/USGS climate data base (solid lines).

Figure 14
Unbiased rms of error (predicted-observed air temperature) as obtained with RACMO for all European synops stations with the old ECHAM4 climate data base (dashed lines) and with the new NOAA/USGS climate data base (solid lines).

Figure 15
Bias (predicted-observed relative humidity) as obtained with RACMO for all European synops stations with the old ECHAM4 climate data base (dashed lines) and with the new NOAA/USGS climate data base (solid lines).

Figure 16
Unbiased rms of error (predicted-observed relative humidity) as obtained with RACMO for all European synops stations with the old ECHAM4 climate data base (dashed lines) and with the new NOAA/USGS climate data base (solid lines).

Figure 17
24hrs accumulated rainfall for the Great Plains test area. Crosses denote no significant rainfall reported (After Jones *et al.*, 1998b).

Figure 18
Average soil moisture content for the West-East transect of the same area as shown in Figure 17, for a (uniformly initialized) control run (upper panel) and an assimilated experimental run (lower panel) for three times of simulation (After Jones *et al.*, 1998b).

Figure 19
Difference between RACMO and METEOSAT surface temperature heating rates for a number of cloud-free synops stations on 25 June 1995, plotted against RACMO forecast error in relative humidity. Shown are results for two runs with RACMO, different with respect to initial soil moisture content. Results for each synops station location are connected with lines.

Figure 20
Bias (prediction-observation) of 2m temperature (a) and specific humidity (b) for the control run (dashed lines) and the run with soil moisture updated using the SEBAL evaporation estimates (solid lines). (after van den Hurk *et al.*, 1998).

TABLE HEADING

Table 1
Parameter ranges used in the adapted TOPUP-SVAT model (taken from McCabe *et al.*,1999)

Figure 1

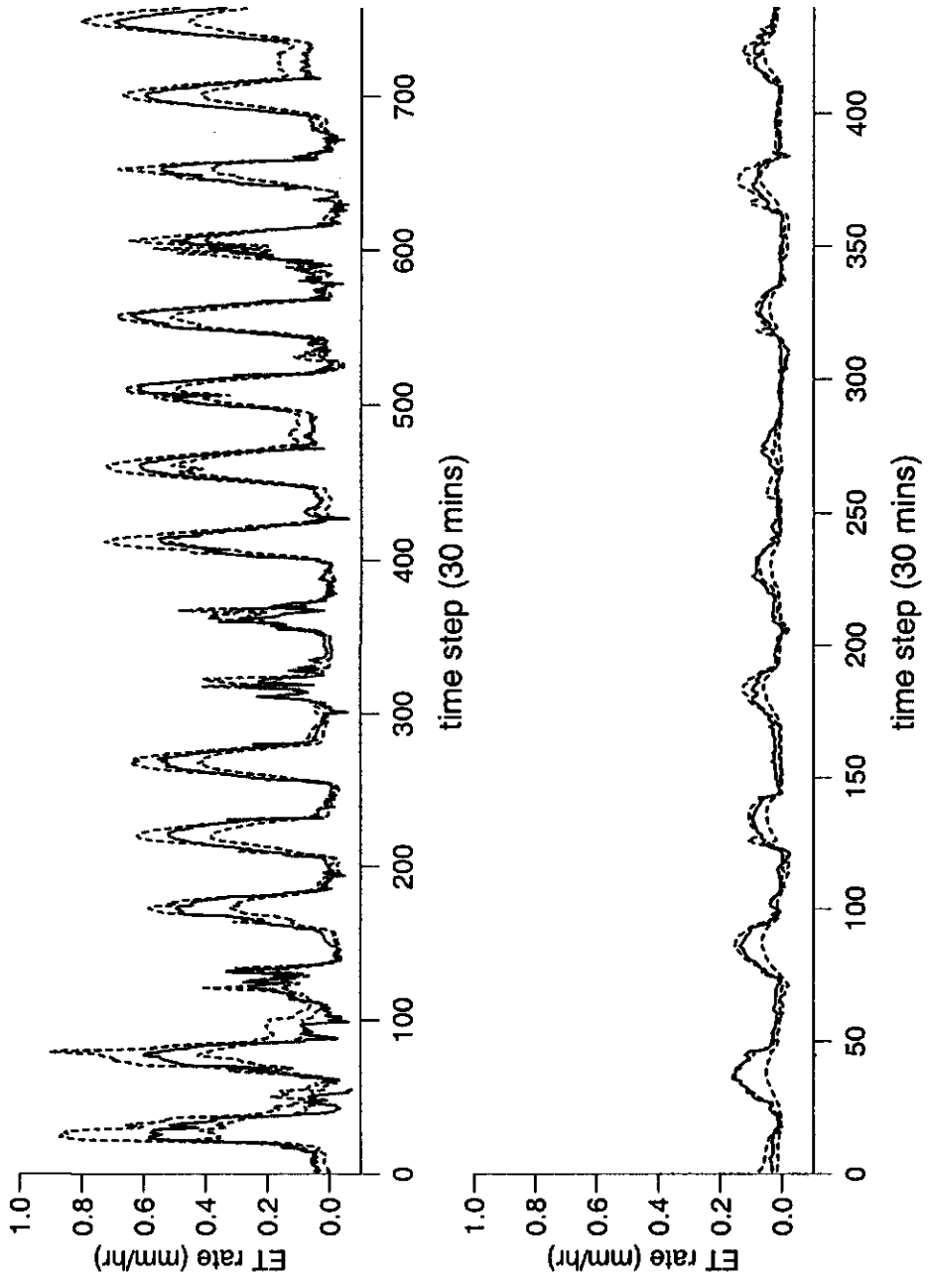
ET rate (mm/hr)
1.0
0.8
0.6
0.4
0.2
0.0
0
100
200
300
400
500
600
700
time step (30 mins)
ET rate (mm/hr)
1.0
0.8
0.6
0.4
0.2
0.0
0
50
100
150
200
250
300
350
400
time step (30 mins)

Figure 2

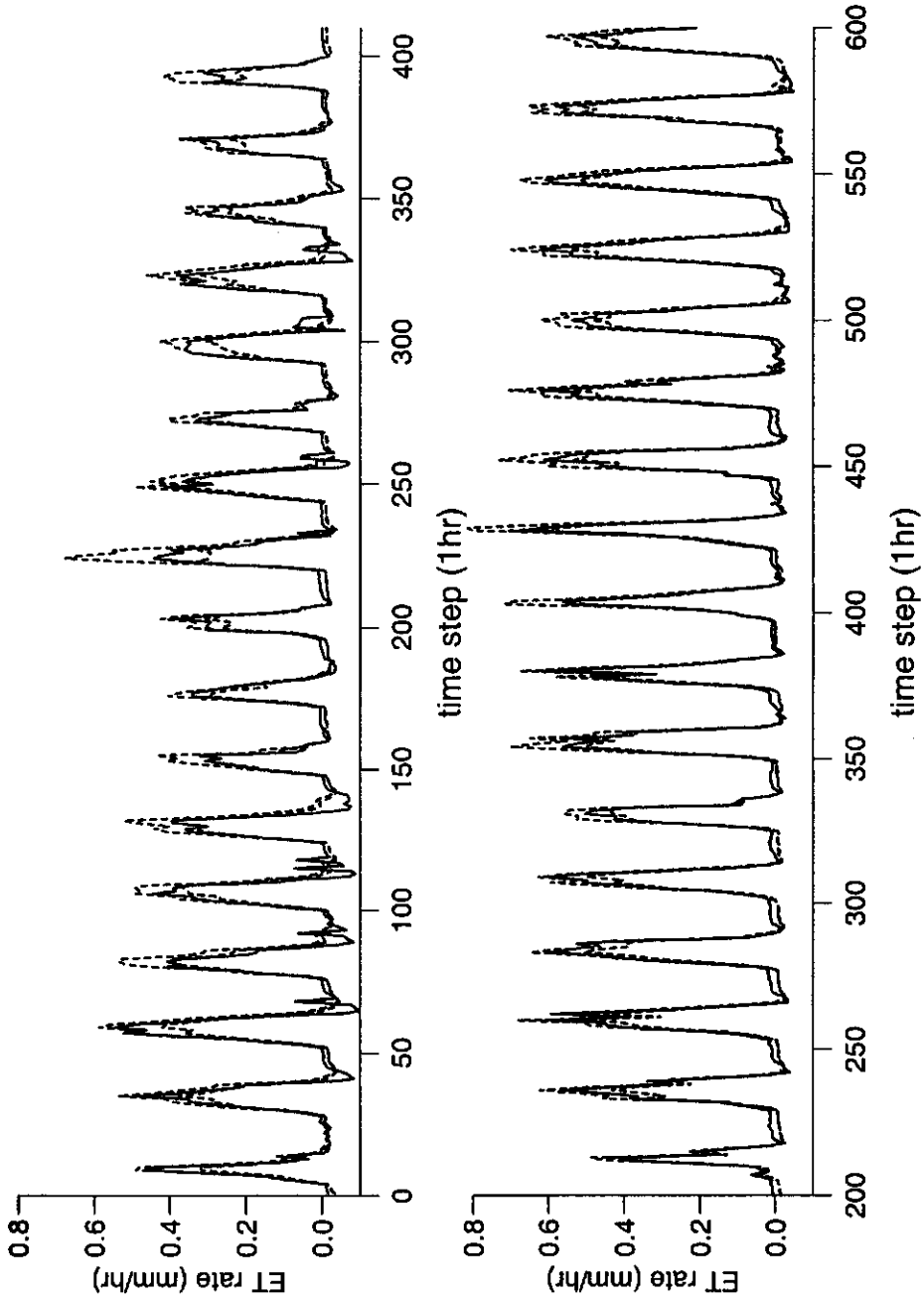
ET rate (mm/hr)
0.0
0.2
0.4
0.6
0.8
0
50
100
150
200
250
300
350
400
time step (1hr)
ET rate (mm/hr)
0.0
0.2
0.4
0.6
0.8
200
250
300
350
400
450
500
550
600
time step (1hr)

Figure 3

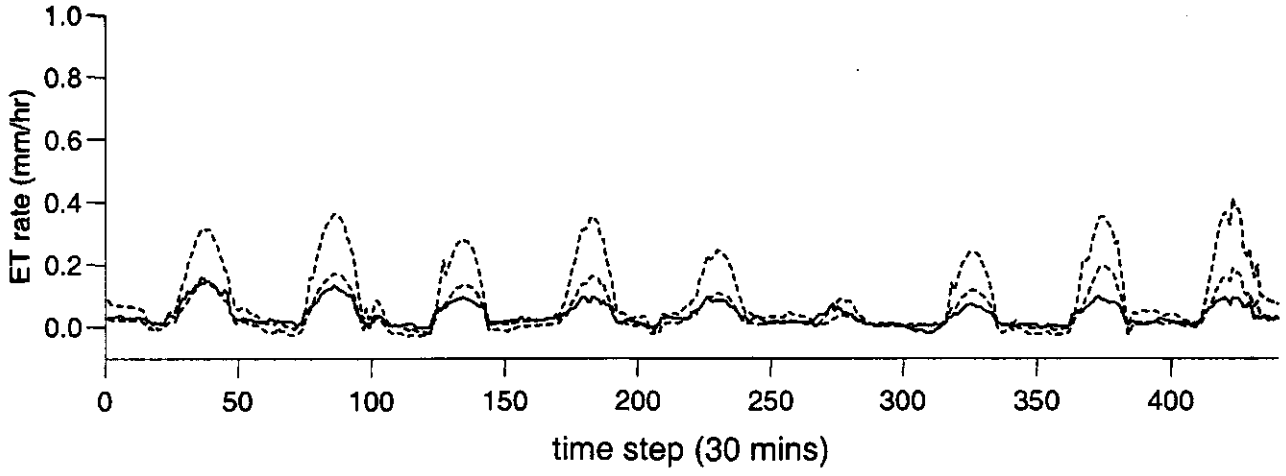

Figure 4

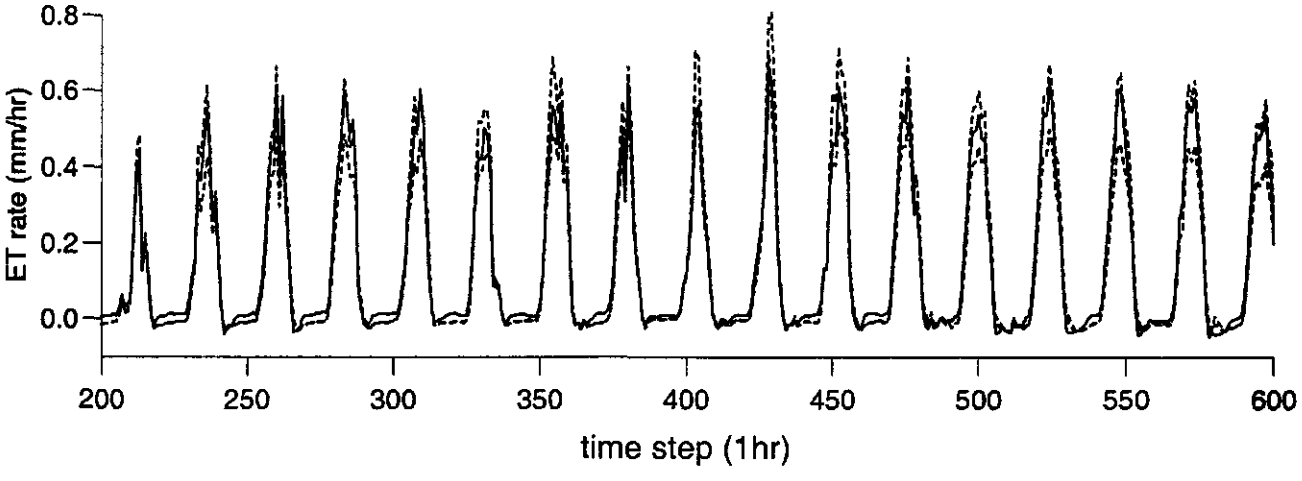

Figure 5

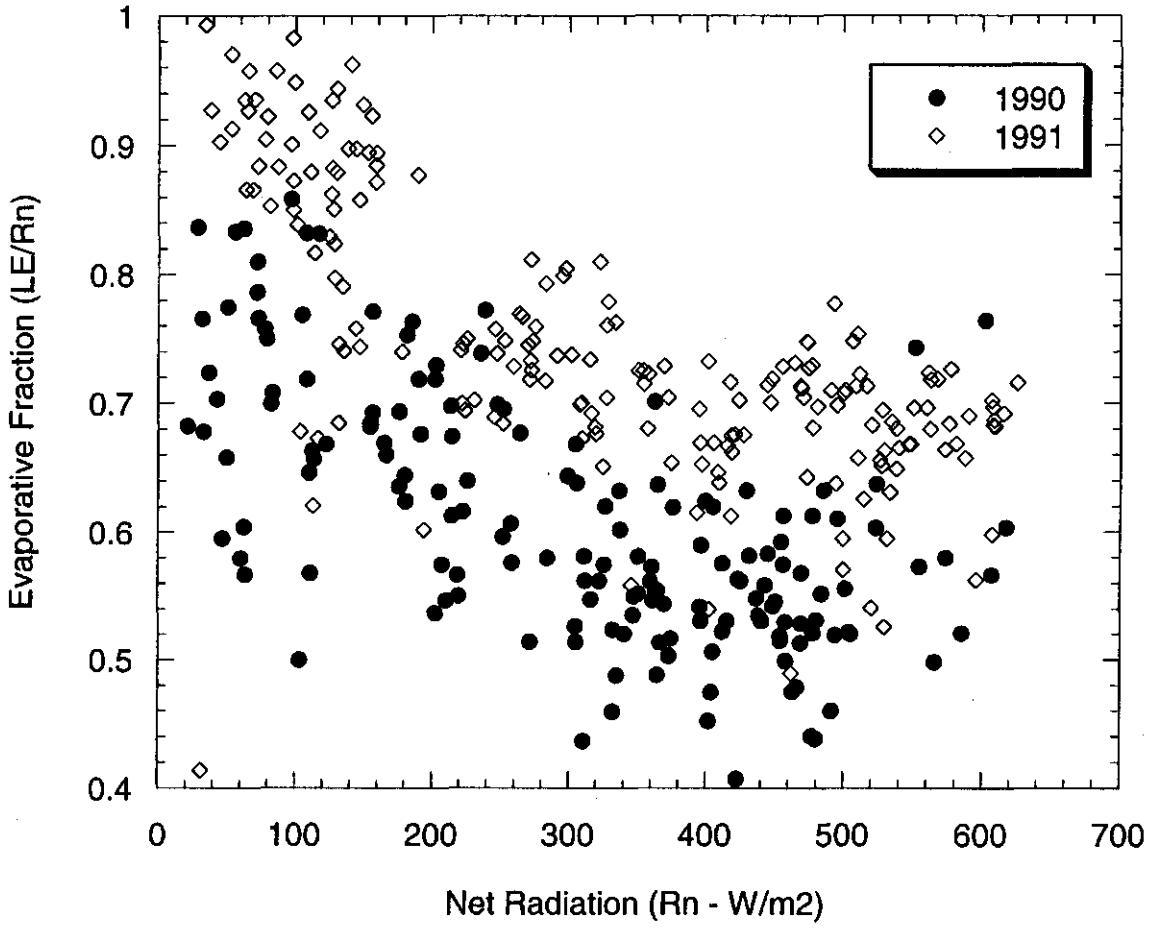
1
0.9
0.8
0.7
0.6
0.5
0.4
0
100
200
300
400
500
600
700
Evaporative Fraction (LE/Rn)
Net Radiation (Rn - W/m2)
1990
1991

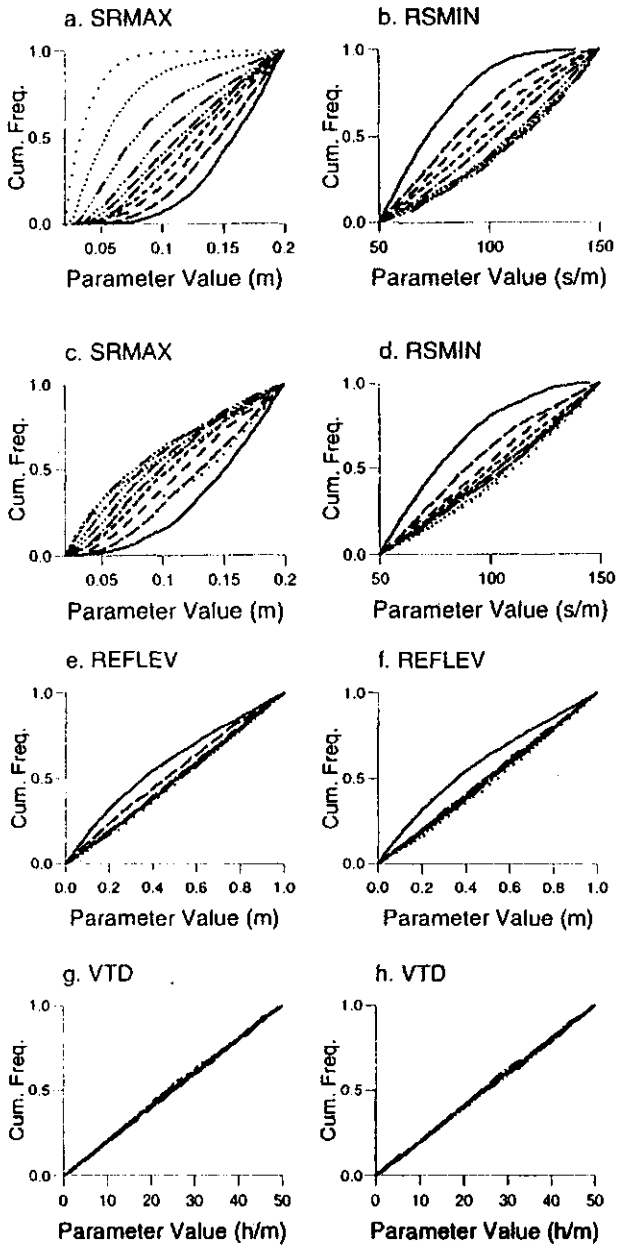

Figure 6

Plots of sensitivity of performance class to model parameters—Set 1 is the lowest performance class, Set 10 is the highest. (a,b) The root zone storage (SRMAX) and the minimum surface resistance (RSMIN) in terms of the cumulative evapotranspiration when driven with the Amazon 1991 data set. (c,d) The root zone storage (SRMAX) and the minimum surface resistance (RSMIN) in terms of the cumulative evapotranspiration when driven with the FIFE IFC-3 data set. (e,f) The reference level for soil transmissivity (REFLEV) with respect to the cumulative evapotranspiration when forced with the FIFE IFC-3 data set, and FIFE IFC-4 data set, respectively. (g,h) The vertical time delay through the unsaturated zone (VTD) for the FIFE IFC-3 data set in terms of cumulative evapotranspiration and efficiency, respectively.

Figure 7

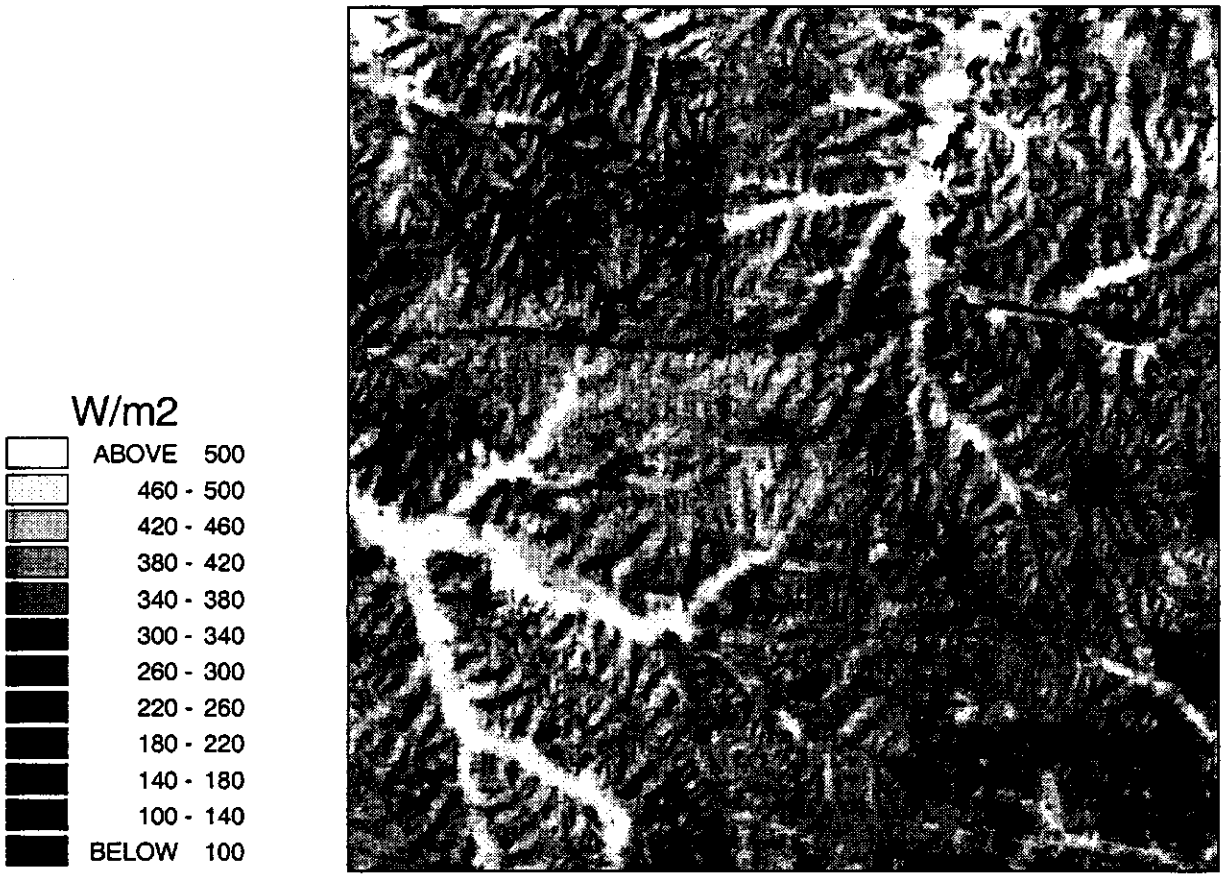
W/m2
ABOVE 500
460 - 500
420 - 460
380 - 420
340 - 380
300 - 340
260 - 300
220 - 260
180 - 220
140 - 180
100 - 140
BELOW 100

Figure 8

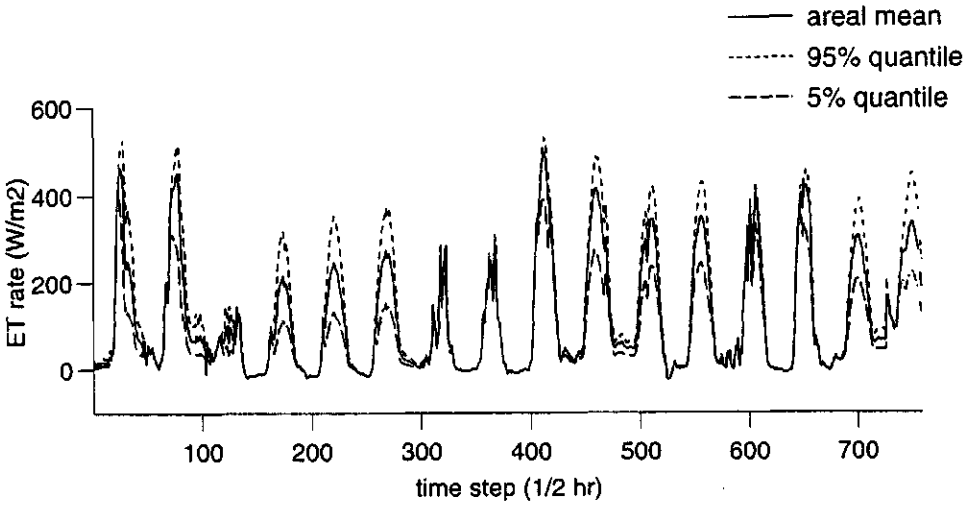

Derived areal mean and 5% and 95% quantiles of the range of fluxes across the FIFE study area.

Figure 9

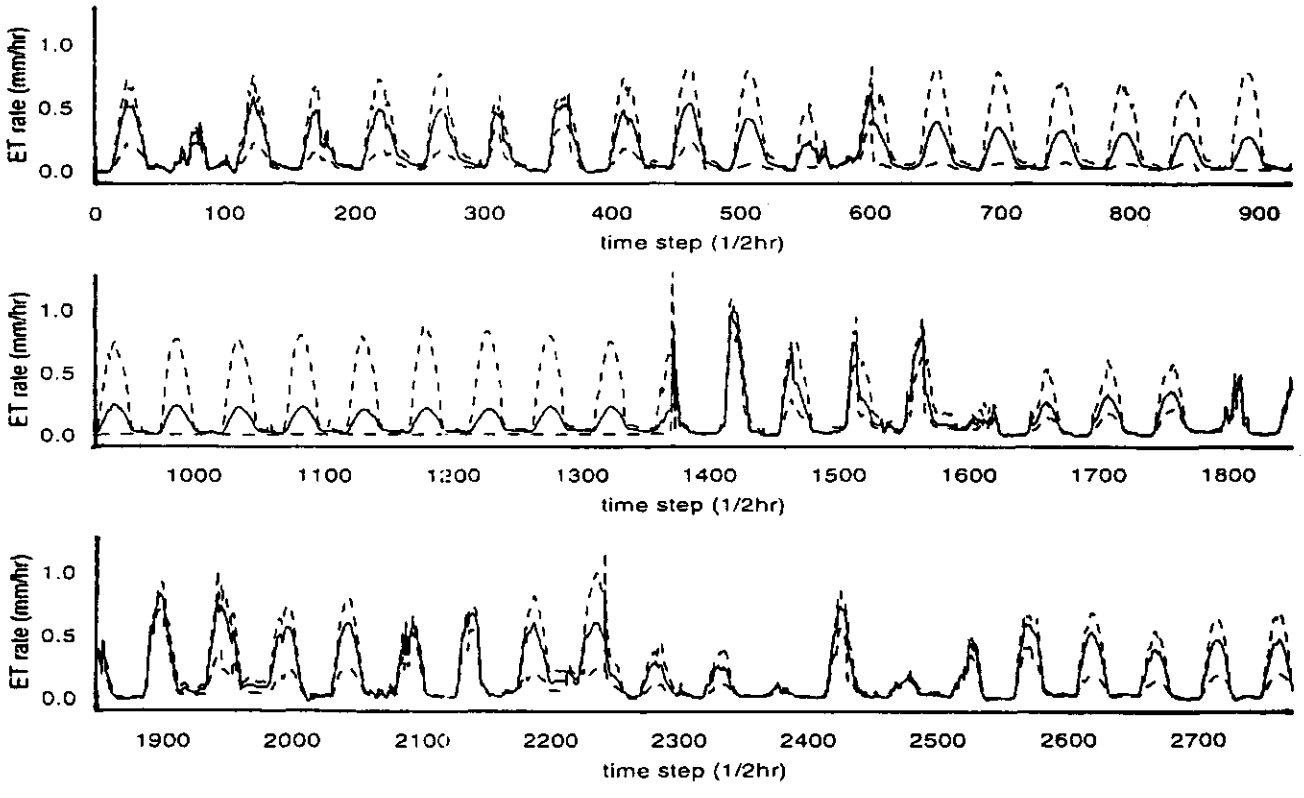

Figure 10

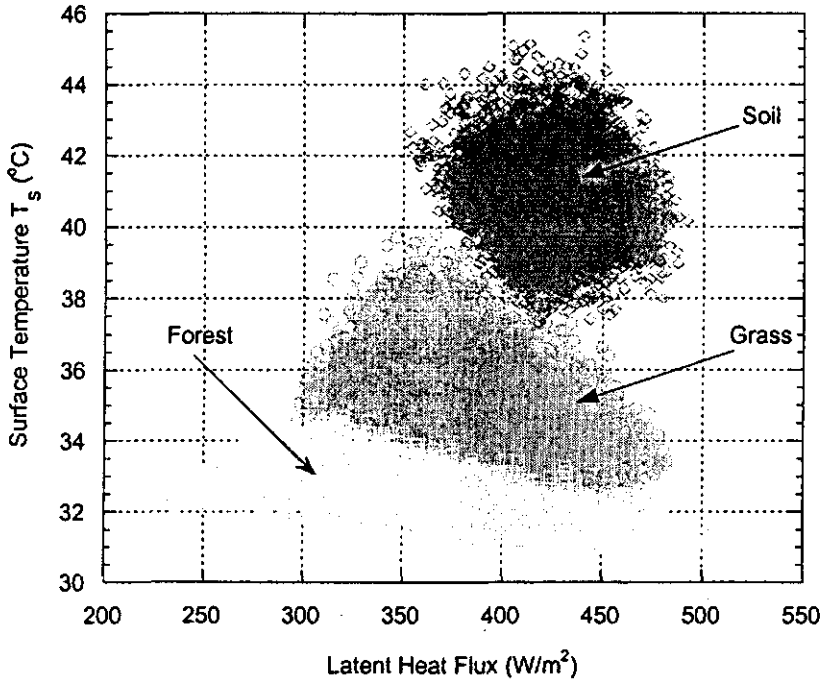
Surface Temperature T_s (°C)
46
44
42
40
38
36
34
32
30
200
250
300
350
400
450
500
550
Latent Heat Flux (W/m^2)
Soil
Forest
Grass

Figure 11

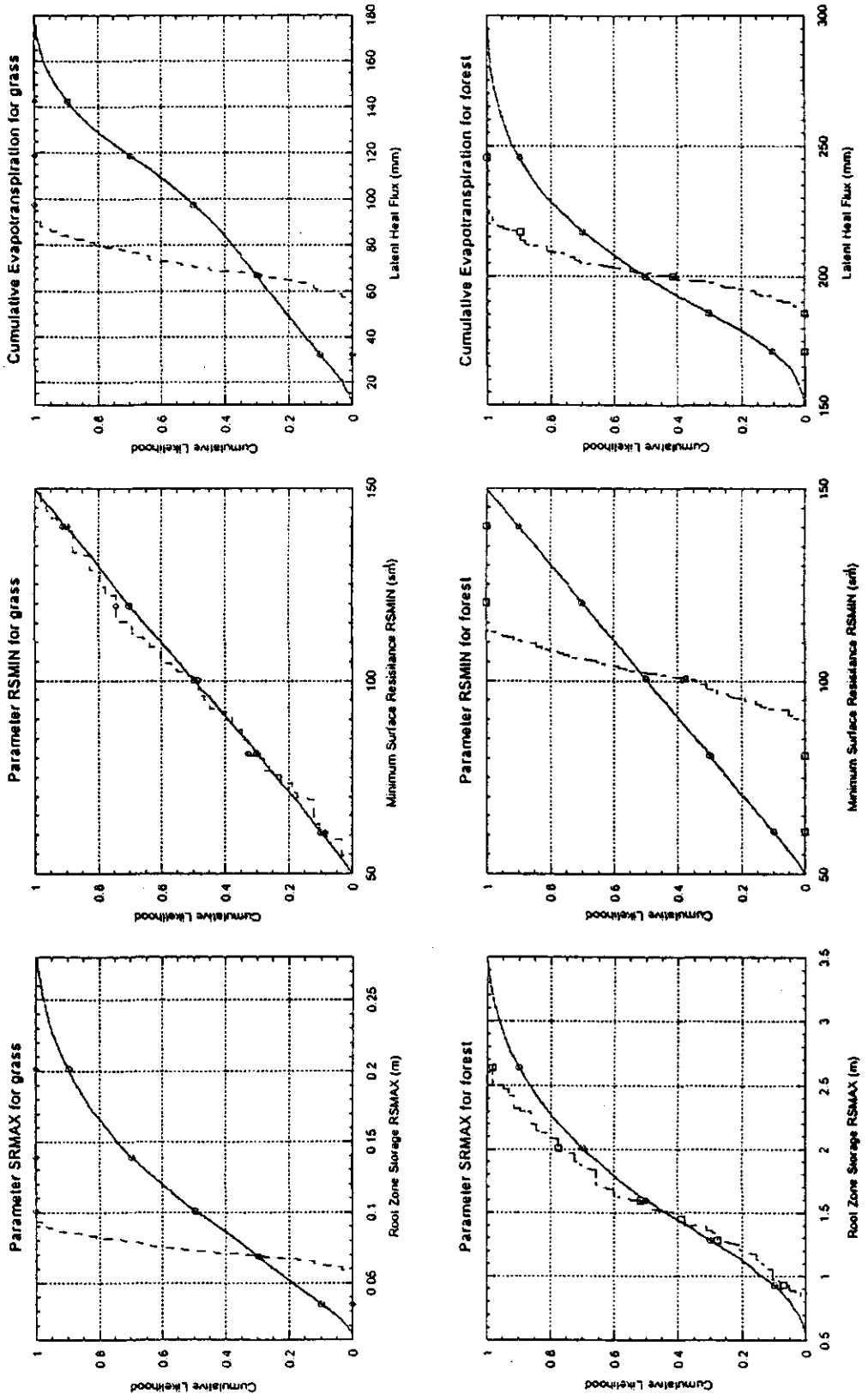
Cumulative Evapotranspiration for grass
Cumulative Likelihood
Latent Heat Flux (mm)
Parameter RSMIN for grass
Minimum Surface Resistance RSMIN (s/m)
Parameter SRMAX for grass
Root Zone Storage RSMAX (m)
Cumulative Evapotranspiration for forest
Parameter RSMIN for forest
Parameter SRMAX for forest

Figure 12

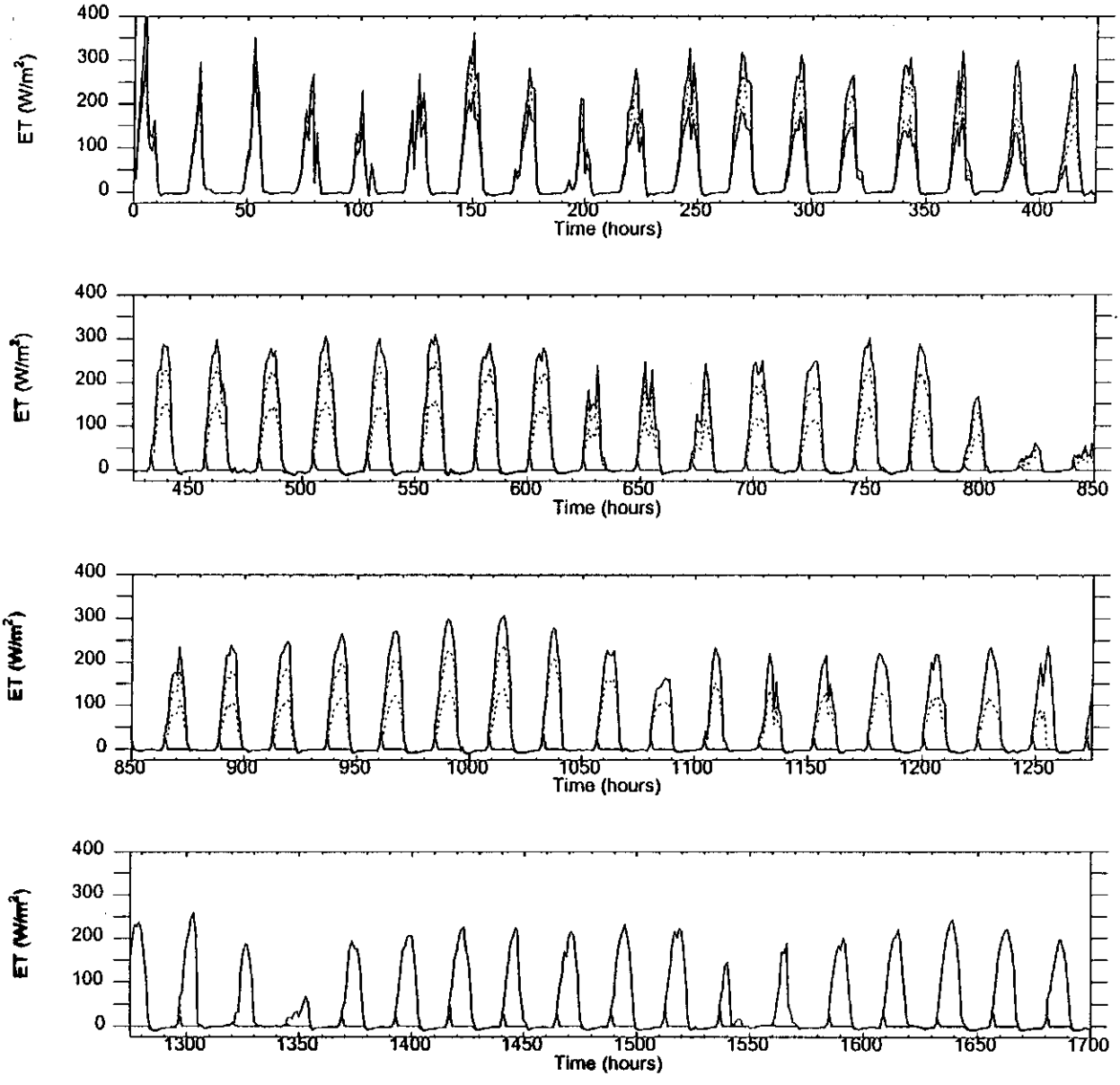
ET (W/m²)
400
300
200
100
0
0
50
100
150
200
250
300
350
400
Time (hours)
ET (W/m²)
400
300
200
100
0
450
500
550
600
650
700
750
800
850
Time (hours)
ET (W/m²)
400
300
200
100
0
850
900
950
1000
1050
1100
1150
1200
1250
Time (hours)
ET (W/m²)
400
300
200
100
0
1300
1350
1400
1450
1500
1550
1600
1650
1700
Time (hours)

Figure 13

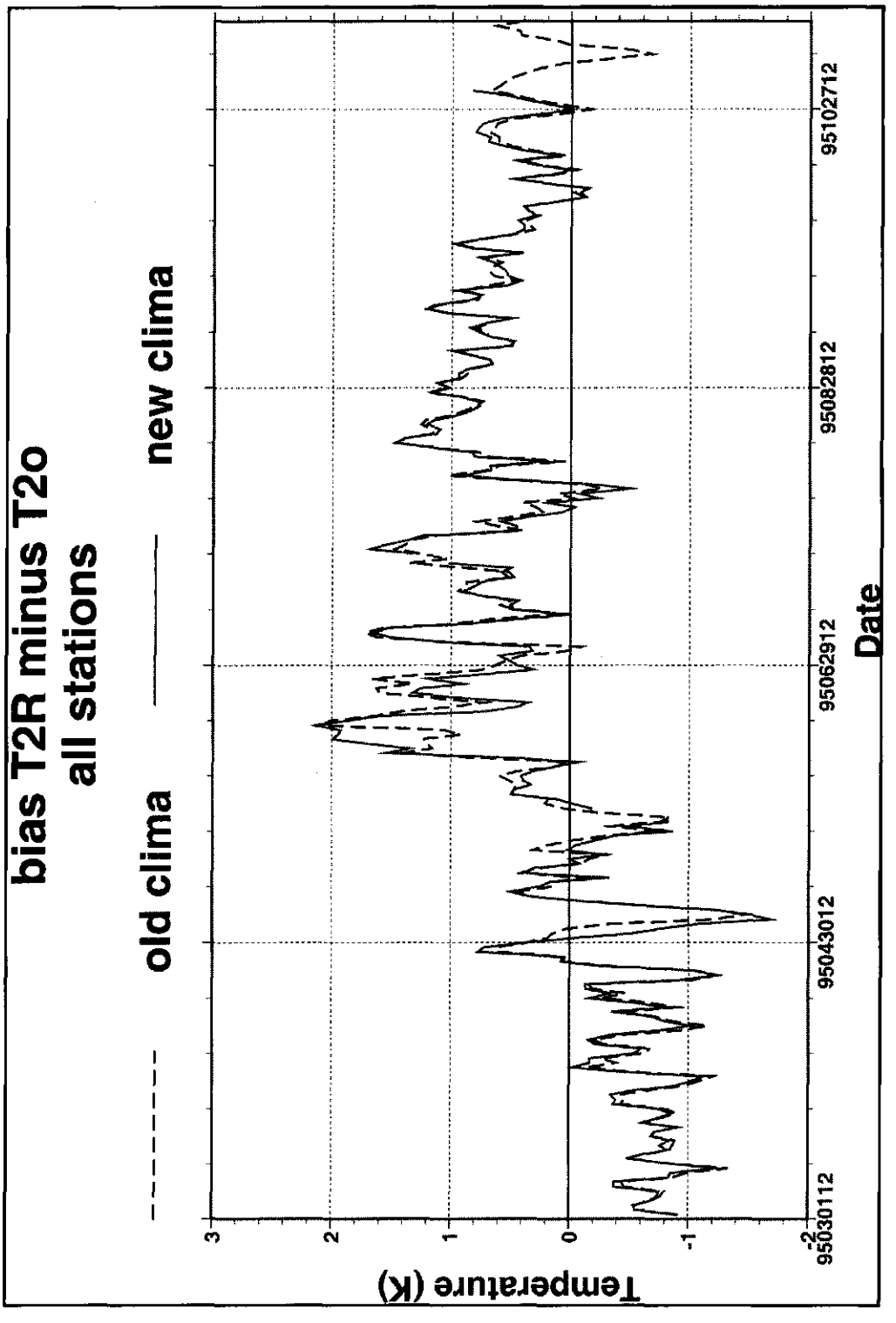
bias T2R minus T2o
all stations
old clima
new clima
Temperature (K)
Date
3
2
1
0
-1
-2
95030112
95043012
95062912
95082812
95102712

Figure 14

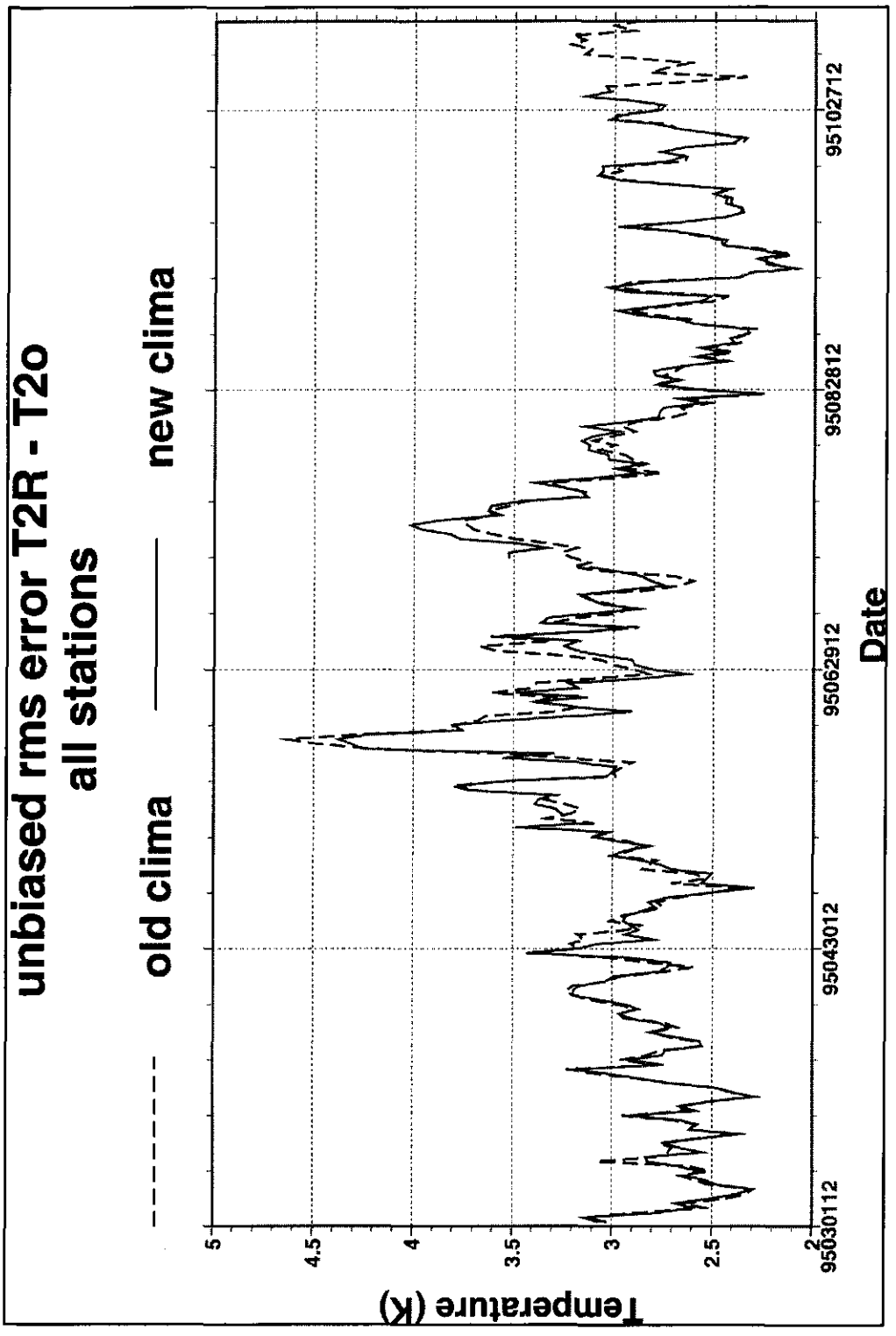
unbiased rms error T2R - T2o
all stations
old clima
new clima
Temperature (K)
5
4.5
4
3.5
3
2.5
2
95030112
95043012
95062912
95082812
95102712
Date

Figure 15

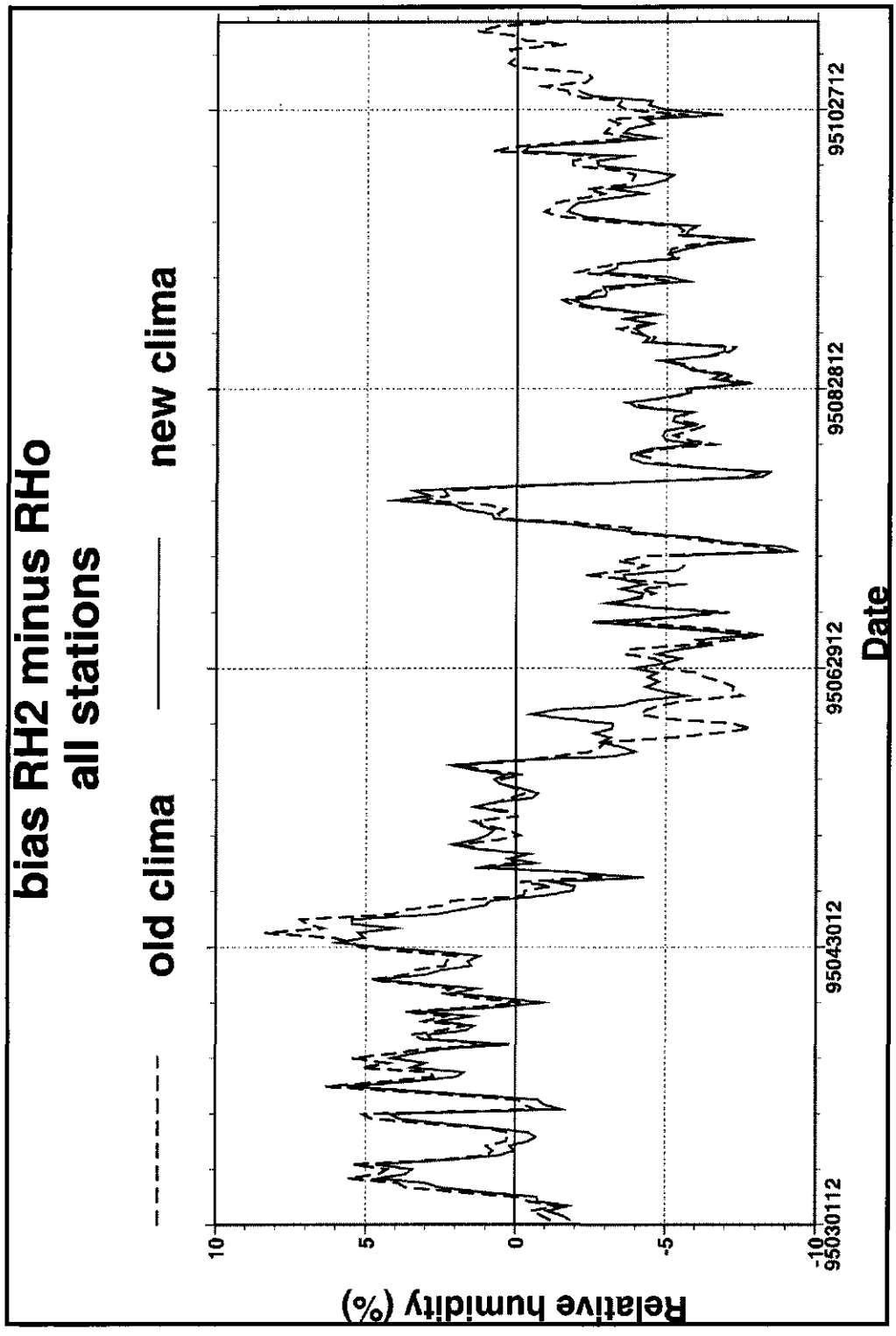
bias RH2 minus RHo
all stations
old clima
new clima
Relative humidity (%)
10
5
0
-5
-10
95030112
95043012
95062912
95082812
95102712
Date

Figure 16

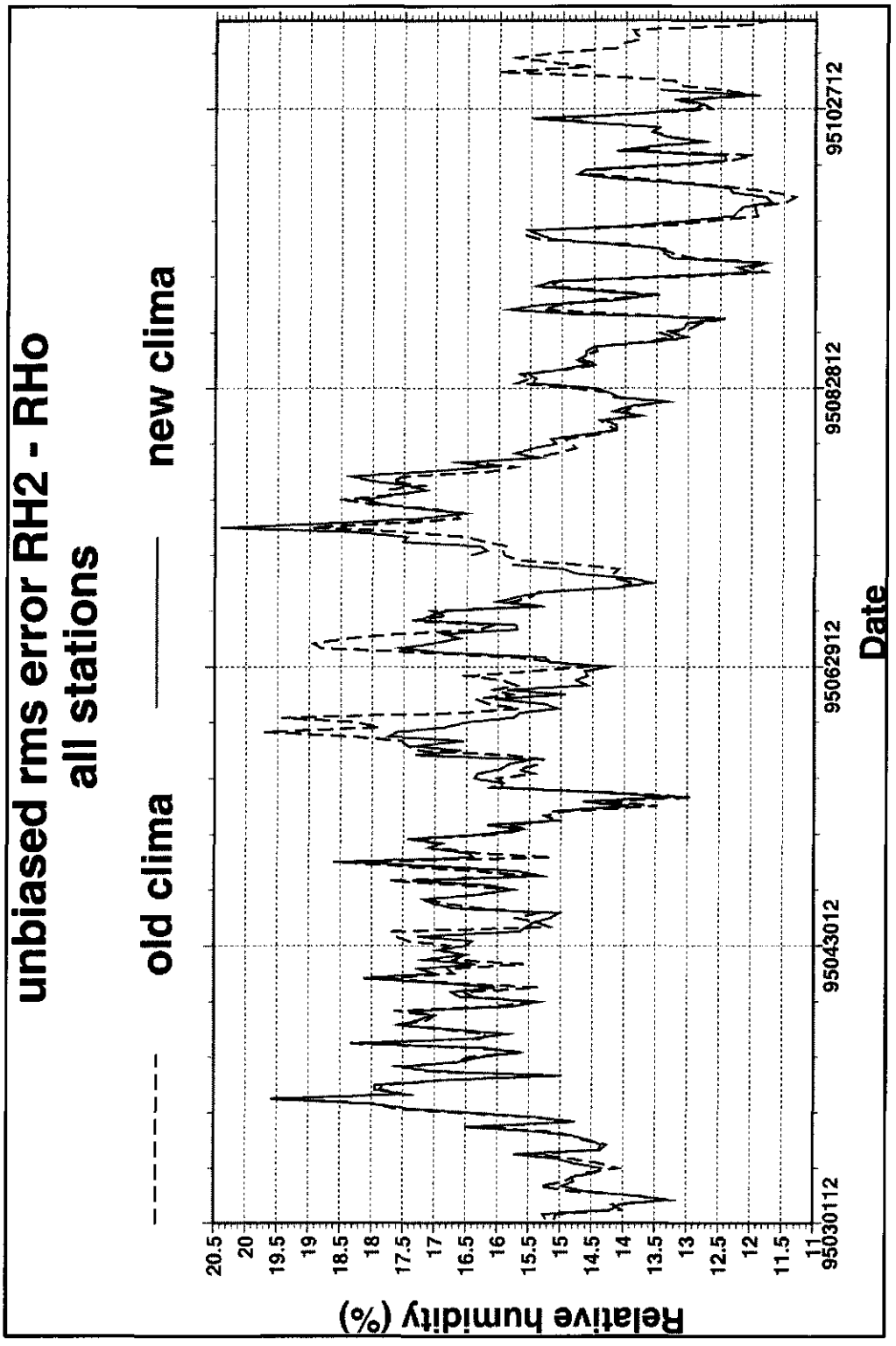
unbiased rms error RH2 - RHo
all stations
old clima
new clima
Relative humidity (%)
Date
20.5
20
19.5
19
18.5
18
17.5
17
16.5
16
15.5
15
14.5
14
13.5
13
12.5
12
11.5
11
95030112
95043012
95062912
95082812
95102712

Figure 17

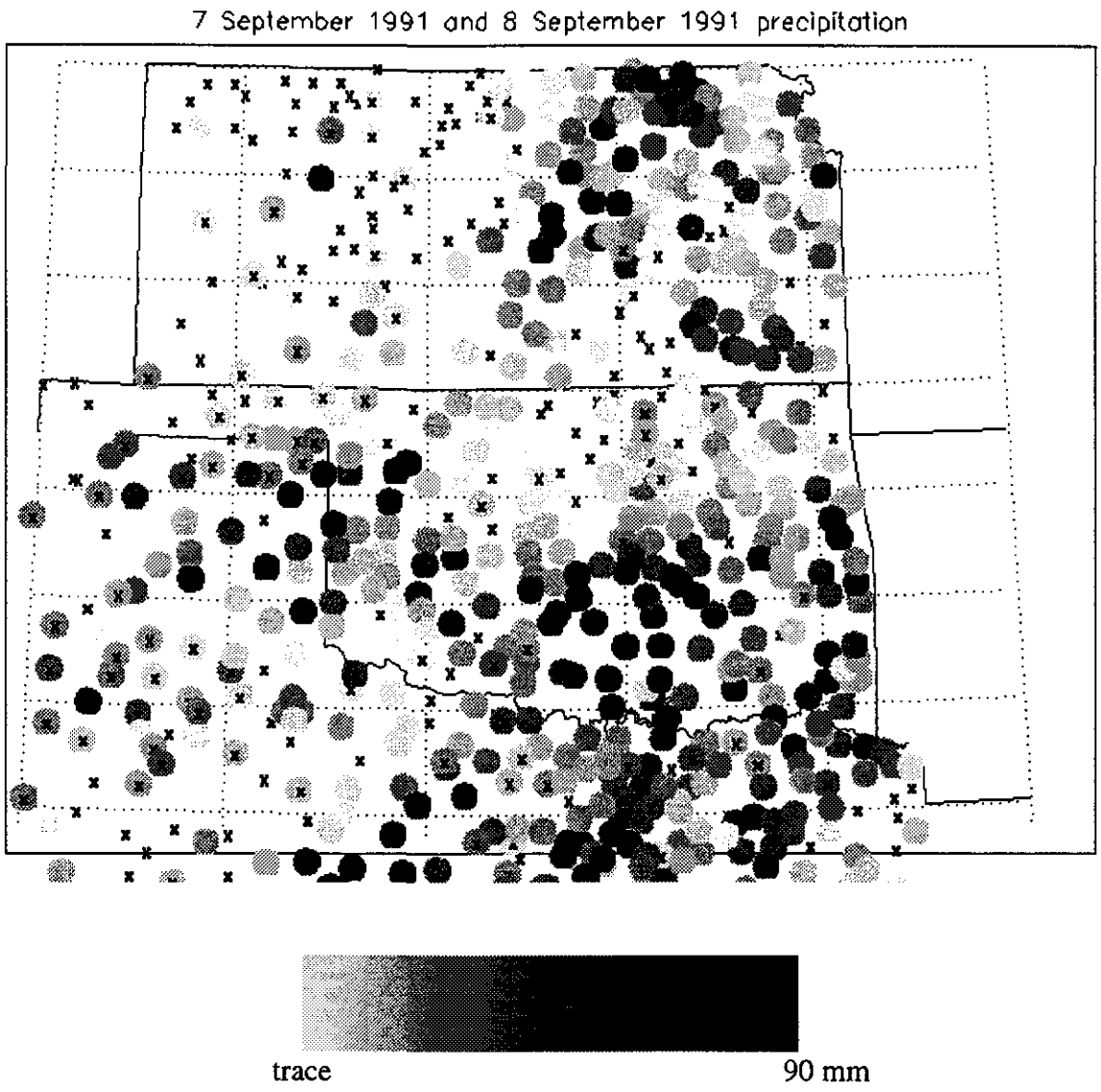
7 September 1991 and 8 September 1991 precipitation
trace
90 mm

Figure 18

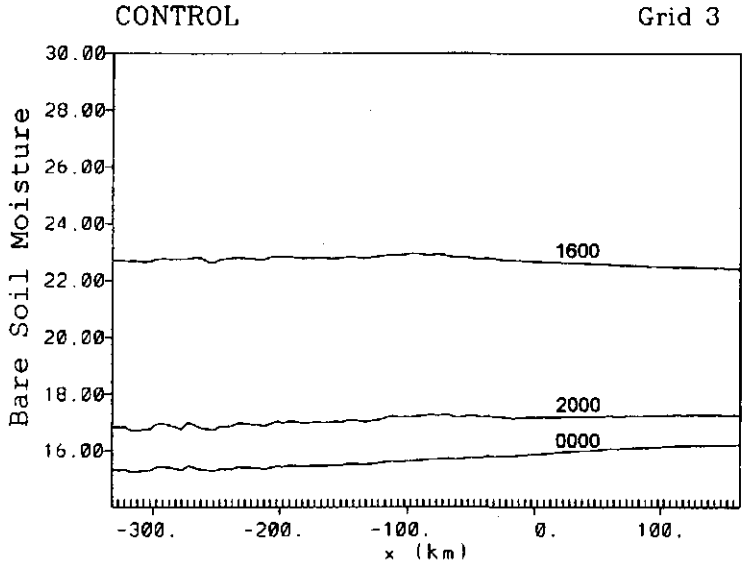
CONTROL
Grid 3
Bare Soil Moisture
30.00
28.00
26.00
24.00
22.00
20.00
18.00
16.00
1600
2000
0000
-300.
-200.
-100.
0.
100.
x (km)

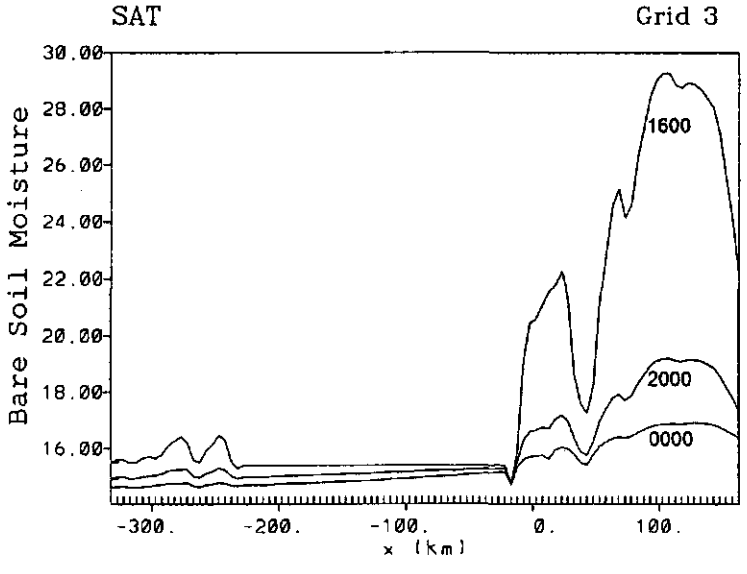
SAT
Grid 3
Bare Soil Moisture
30.00
28.00
26.00
24.00
22.00
20.00
18.00
16.00
1600
2000
0000
-300.
-200.
-100.
0.
100.
x (km)

Figure 19

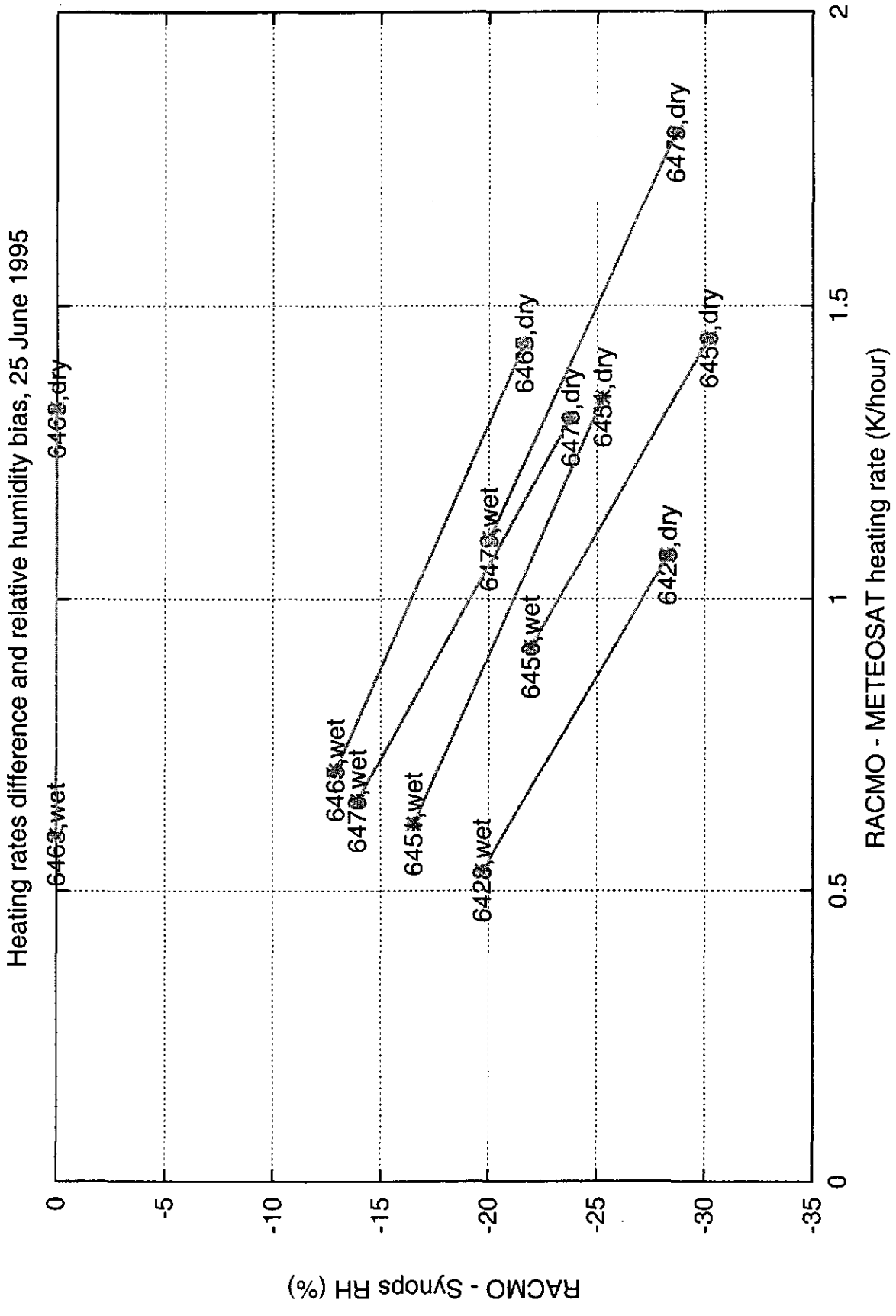
Heating rates difference and relative humidity bias, 25 June 1995
RACMO - METEOSAT heating rate (K/hour)
RACMO - Synops RH (%)
0
-5
-10
-15
-20
-25
-30
-35
0
0.5
1
1.5
2
6463,wet
6463,dry
6465,wet
6465,dry
6478,wet
6478,dry
6458,wet
6458,dry
6453,wet
6453,dry
6423,wet
6423,dry

Figure 20A

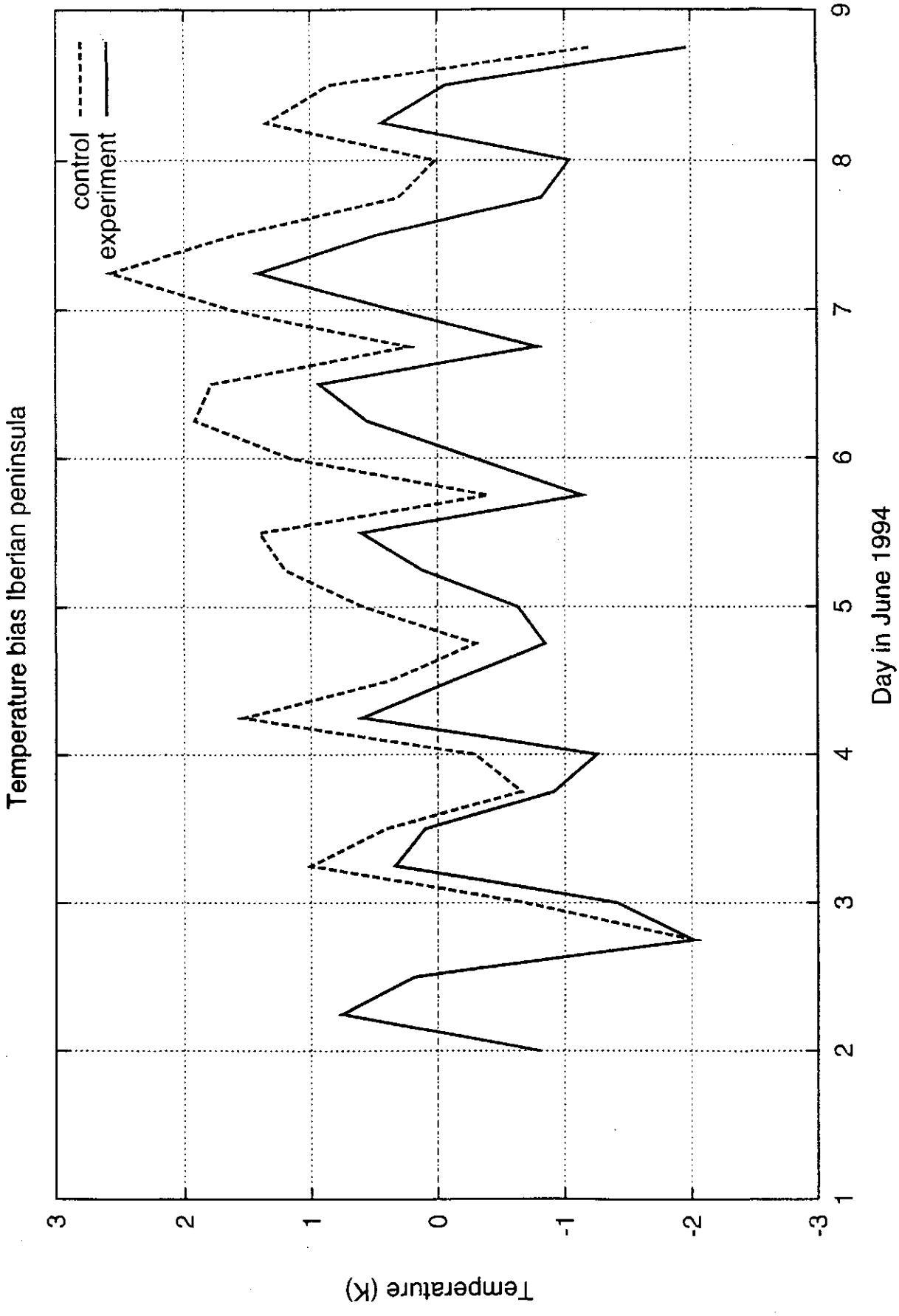
Temperature bias Iberian peninsula
control
experiment
Temperature (K)
3
2
1
0
-1
-2
-3
1
2
3
4
5
6
7
8
9
Day in June 1994

Figure 20B

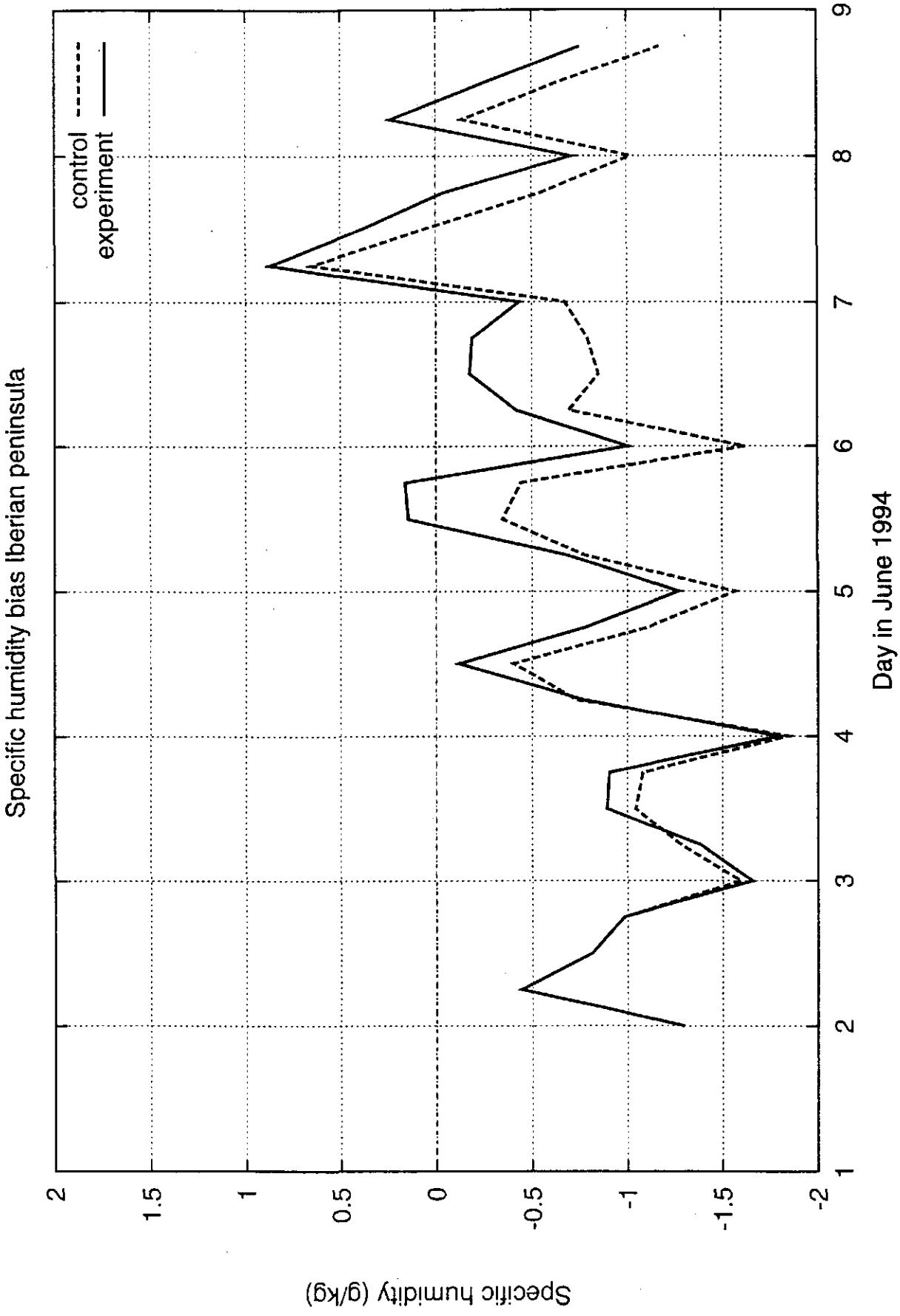
Specific humidity bias Iberian peninsula
control
experiment
Specific humidity (g/kg)
Day in June 1994
2
1.5
1
0.5
0
-0.5
-1
-1.5
-2
1
2
3
4
5
6
7
8
9

Table 1

Table 1: Parameter ranges used in the TOPUP-SVAT model.

Varied Parameters		Parameter Ranges		
		Soil	*Grass*	*Forest*
h_c	canopy height (m)	0	0.1 – 1	5 – 12
β	% net radiation returned as ground heat flux	←	0.15 – 0.25	→
RSMIN	minimum surface resistance (sm^{-1})	←	50 – 150	→
RSMAX	maximum surface resistance (sm^{-1})	←	300 – 1000	→
$\ln(z_0/z_h)$	ratio of z_0 for momentum & heat flux	←	1 – 3	→
SRMAX	root zone storage (m)	0.01 – 0.1	← 0.1 h_c – 0.3 h_c →	
z_0	roughness length for momentum flux	< 0.0005	← γ (h_c -d) →	
D	zero displacement height	0	← 0.6 h_c – 0.7 h_c →	
γ	coefficient used in z_0 calculation	-	← 0.2 – 0.4 →	